Large-scale deorphanization of *Nematostella vectensis* neuropeptide GPCRs supports the independent expansion of bilaterian and cnidarian peptidergic systems

Authors:

Daniel Thiel[1,*,†], Luis Alfonso Yañez-Guerra[1,5†], Amanda Kieswetter[2], Alison G. Cole[3], Liesbet Temmerman[2], Ulrich Technau[3], Gáspár Jékely[1,4,*]

[1] Living Systems Institute, University of Exeter, Stocker Road, Exeter, UK
[2] Animal Physiology & Neurobiology, Department of Biology, University of Leuven (KU Leuven), Leuven, Belgium
[3] Department of Neurosciences and Developmental Biology, Faculty of Life Sciences, University of Vienna, Vienna, Austria
[4]Centre for Organismal Studies (COS), University of Heidelberg, 69120 Heidelberg, Germany
[5]Current affiliation: School of Biology, Institute for Life Sciences, University of Southampton, University Road SO17 1BJ, Southampton, UK

[†]These authors contributed equally
*Correspondence: d.thiel@exeter.ac.uk, gaspar.jekely@cos.uni-heidelberg.de

Abstract

Neuropeptides are ancient signaling molecules in animals but only few peptide receptors are known outside bilaterians. Cnidarians possess a large number of G protein-coupled receptors (GPCRs) – the most common receptors of bilaterian neuropeptides – but most of these remain orphan with no known ligands. We searched for neuropeptides in the sea anemone *Nematostella vectensis* and created a library of 64 peptides derived from 33 precursors. In a large-scale pharmacological screen with these peptides and 161 *N. vectensis* GPCRs, we identified 31 receptors specifically activated by one of 14 peptides. Mapping GPCR and neuropeptide expression to single-cell sequencing data revealed how cnidarian tissues are extensively connected by multilayer peptidergic networks. Phylogenetic analysis identified no direct orthology to bilaterian peptidergic systems and supports the independent expansion of neuropeptide signaling in cnidarians from a few ancestral peptide-receptor pairs.

Introduction

The origin of neuropeptides predates the emergence of neurons and it is believed that these signaling molecules have been utilized in the most ancestral nervous systems (Jékely, 2021;

Moroz et al., 2021; Yañez-Guerra et al., 2022). Neuropeptide-like molecules occur in all major animal clades with neurons, the Bilateria, Cnidaria and Ctenophora, and even in the neuron-less Placozoa and Porifera (Hayakawa et al., 2022; Koch and Grimmelikhuijzen, 2019; Nikitin, 2015; Sachkova et al., 2021; Yañez-Guerra et al., 2022). However, the deep relationships of animal neuropeptidergic systems, in particular between Bilateria and non-bilaterians, have remained elusive.

Most mature bioactive neuropeptides are 3-20 amino acids long and derive from longer proneuropeptide precursors through cleavage and other post-translational modifications. The same set of enzymes are involved in proneuropeptide processing across animals. These include prohormone convertases, which recognize dibasic cleavage sites flanking the active peptides, and peptidyl-glycine alpha-amidating monooxygenase (PAM), which converts C-terminal glycine residues to amide groups (Chufán et al., 2009; Seidah, 2011). Proneuropeptide precursors can contain a single peptide or multiple copies of identical or divergent peptide sequences separated by cleavage sites. The often repetitive structure and the presence of short active sequences interspersed with less-constrained interpeptide regions allow propeptide sequences to evolve relatively rapidly. Consequently, with increasing evolutionary distances it often becomes hard or impossible to recognize orthologous proneuropeptide sequences. Even within Bilateria, the orthology relationship of many neuropeptide families between protostomes and deuterostomes have only been recognized due to the orthology of their receptors (e.g., vertebrate orexin and insect allatotropin) (Alzugaray et al., 2019; Elphick et al., 2018; Mirabeau and Joly, 2013; Semmens et al., 2015).

Most neuropeptides signal through G protein-coupled receptors (GPCRs), which are larger seven-transmembrane proteins that show a slower evolutionary rate than proneuropeptide precursors. The cases where the evolution of both the proneuropeptides and their receptors could be reconstructed, revealed a strong pattern of coevolution between receptor and ligand (Elphick et al., 2018; Escudero Castelán et al., 2022; Grimmelikhuijzen and Hauser, 2012; Jékely, 2013; Mirabeau and Joly, 2013; Yañez-Guerra and Elphick, 2020). This coevolutionary pattern has been used to also trace the evolution of peptide families where the ligands are too divergent to retain phylogenetic signal. These analyses revealed more than 30 conserved peptidergic signaling systems across bilaterians (Elphick et al., 2018; Jékely, 2013; Mirabeau and Joly, 2013; Thiel et al., 2021; Yañez-Guerra et al., 2022).

The nervous system of cnidarians has long been known to be strongly peptidergic and proneuropeptides have been found across all major cnidarian clades (Koch et al., 2021; Koch and Grimmelikhuijzen, 2020, 2019). Most cnidarian neuropeptides are short amidated peptides, resembling those found in bilaterians. Genomic comparisons revealed three proneuropeptide families that were present in the cnidarian stem lineage. All three give rise to short amidated neuropeptides: GLWamides, GRFamides, and PRXamides (with "X" representing a variable amino acid residue) (Koch et al., 2021; Koch and Grimmelikhuijzen, 2020, 2019). Other neuropeptides are more specific to certain cnidarian groups such as QITRFamide and HIRamide to Hexacorallia or LRWamides to Anthozoa (Koch and Grimmelikhuijzen, 2020). Peptides that are sufficiently similar to be considered orthologous between bilaterians and cnidarians are restricted to a few atypical neuropeptides. These include insulin-related peptides, glycoprotein-hormone-related peptides, trunk related peptides, nesfatin, and phoenixin (de Oliveira et al., 2019; Roch and Sherwood, 2014; Yañez-Guerra et al., 2022). The more common

short amidated peptides, however, have no clear orthologs in bilaterians. Similarity is at most restricted to one or two C-terminal residues, such as between RFamide or Wamide peptides (Walker et al., 2009; Williams, 2020); (Jékely, 2013). Sometimes this has been interpreted as evidence of common origin but there is no other evidence supporting potential orthologies for these cnidarian peptides and their bilaterian counterparts. Receptors for most cnidarian neuropeptides are still unknown, with two exceptions. These include receptors for *Hydra vulgaris* RFamide peptides and a receptor for a PRXamide maturation-inducing hormone (MIH) in the hydrozoan *Clytia hemisphaerica* (Artigas et al., 2020; Assmann et al., 2014). *Hydra* RFamide peptides activate heterotrimeric peptide-gated ion channels belonging to the DEG/ENaC family and distantly related to bilaterian RFamide- and Wamide-gated ion channels (Dandamudi et al., 2022; Elkhatib et al., 2022; Gründer et al., 2022). The *Clytia* MIH receptor is a class A GPCR, which together with related cnidarian GPCRs shows a many-to-many ortholog relationship to a range of bilaterian neuropeptide GPCR families that also contain receptors for RFamide-like neuropeptides (Artigas et al., 2020).

Cnidarian genomes can encode a large number of class A GPCRs. The genome of the sea anemone *Nematostella vectensis* for example contains over 1000 GPCR genes (Krishnan and Schiöth, 2015). Earlier analyses suggested direct orthologous relationships between several cnidarian and bilaterian neuropeptide GPCRs such as orexin/allatotropin, somatostatin or neuropeptide Y receptors, beside others (Alzugaray et al., 2013; Anctil, 2009; Krishnan and Schiöth, 2015). However, these results were either only based on BLAST similarity, or limited phylogenetic analyses. More recent and comprehensive phylogenies suggest that cnidarian neuropeptide GPCRs are more closely related to each other than to bilaterian neuropeptide GPCRs and only show many-to-many, or few-to-many orthology with bilaterian receptors (Artigas et al., 2020; Hauser et al., 2022; Thiel et al., 2018). However, a comprehensive phylogenetic analysis of cnidarian GPCRs is still lacking. This, together with the paucity of experimentally characterized receptors, leaves our understanding of the evolution of eumetazoan peptidergic systems fragmentary.

Here, in a large-scale bioinformatic analysis, we map the global sequence diversity of metazoan class A GPCRs to identify neuropeptide GPCR candidates in cnidarians. We then use mass spectrometry and bioinformatics to compile a library of predicted *N. vectensis* neuropeptides. In a combinatorial pharmacological ligand-receptor assay, we test our peptide library against selected *N. vectensis* GPCRs and identify 31 neuropeptide receptors. By phylogenetic analysis, we reconstruct ancestral cnidarian GPCR A systems and their relationship to bilaterian systems. Finally, we map proneuropeptide and GPCR expression to a single-cell RNAseq dataset (Cole et al., 2024) to analyze tissue-level peptidergic signaling in *N. vectensis*. Our results reveal extensive peptidergic networks in *N. vectensis* and support the independent expansion of neuropeptide signaling in Cnidaria and Bilateria.

Results and Discussion

Creation of a *Nematostella* neuropeptide library

To obtain a comprehensive library of endogenous neuropeptides in *N. vectensis,* we extended the list of known proneuropeptides (Hayakawa et al., 2019; Koch and Grimmelikhuijzen, 2020) by mass spectrometry and bioinformatic screening (Figure 1A). We first screened a *N. vectensis* transcriptome collection for sequences encoding a signal peptide. This predicted secretome was filtered with regular expressions to detect sequences with the repetitive dibasic cleavage sites (K and R in any combination) and amidation sites, using a custom script from a previous publication (Thiel et al., 2021). In addition, we used standard BLAST searches using known cnidarian neuropeptide precursors. In parallel, we analyzed methanolic extracts from *N. vectensis* larval, juvenile and adult tissue by mass spectroscopy (LC-MS/MS) (Figure 1–figure supplement 1). The LC-MS/MS analysis confirmed the existence of peptides predicted from various precursor sequences (Supplementary file 1, 2). It also confirmed the existence of two different precursors that encode the FLRNamide peptide and two different precursors that encode the LRWamide1 peptide, by identifying non-amidated peptides that are encoded between cleavage sites next to the name-giving peptides LRWamide and FLRNamide (Figure 1C, Supplementary file 1,2) (Koch and Grimmelikhuijzen, 2020).
MS confirmed the occurrence of N-terminal peptide cleavage at dibasic KR-x, RR-x and KK-x sites, with "x" indicating the N-terminal amino acid of the resulting active peptide (Figure 1B, Supplementary file 1). Cleavage at such dibasic sites is typical for bilaterian precursors (Southey et al., 2008; Veenstra, 2000). In *Nematostella*, the cleavage site is often followed by a -Q residue as the most N-terminal amino acid of the peptide (Figure 1B). Cleavage at dibasic sites, however, does not occur in all precursors. Our MS data showed that some peptides are processed by cleavage N-terminal to a Q residue without any basic residue but the cleavage site is instead often accompanied by an acidic (D or E) residue 1 or 2 positions N-terminally of the cleavage site (Figure 1B, Supplementary file 1). Another motif includes two proline residues in position 2 and 3 from the N-terminus of the peptide, and in some cases a single proline in either the 2nd or 3rd position (Figure 1B, Supplementary file 1). These proline-related cleavage sites are also often accompanied by an acidic residue flanking the peptide N-terminal of the cleavage site. Such non-dibasic cleavage sites have previously been proposed for Cnidaria (Hayakawa et al., 2022, 2019; Koch and Grimmelikhuijzen, 2019). Some precursors, such as the one for HIRamide, also showed alternative N-terminal cleavage of the same peptide copy, resulting in different versions of the same peptide (Figure 1–figure supplement 1, Supplementary file 1), indicating stepwise cleavage or controlled degradation of peptides.
C-terminal peptide cleavage occurs at dibasic x-KR, x-RR, x-KK and in some cases at alternative monobasic Rxx-R sites, with a second basic amino acid 3 positions N-terminal of the cleavage site (Figure 1B, Supplementary file 1). This is similar to the C-terminal cleavage found in bilaterian propeptides (Southey et al., 2008; Veenstra, 2000). In many neuropeptides, we could also confirm peptide alpha-amidation by the conversion of a C-terminal glycine residue to an amide group.

Based on the MS data, we included the additional, non-dibasic N-terminal cleavage sites into our script that uses regular expressions to search for repetitive cleavage sites (Thiel et al., 2024) and re-screened the predicted secretome. With our combined approach, we could identify novel neuropeptide precursors, verify the processing of known neuropeptide precursors and refine cleavage site predictions. We used this information to prepare a list of 33 *N. vectensis* proneuropeptides, excluding potential isoforms of the same precursor but including 2 potential paralogs of the FLRNamide, LRWamide1, and pyrQITRFamide peptide precursors (Supplementary file 2). Our screen complements the list of known neuropeptides in *N. vectensis* (Hayakawa et al., 2022, 2019; Koch and Grimmelikhuijzen, 2020) with 15 new neuropeptide precursors. However, our list did not contain the recently identified GGYamide, GTEamide and IVLamide peptides (Hayakawa et al., 2022) or bursicon- and insulin-like peptides.
We inspected all precursors individually and predicted signal peptides, cleavage sites and amidation sites (Figure 1C, Supplementary file 2). Based on our cleavage-site predictions we then compiled a library of 64 synthetic *Nematostella* neuropeptides, including different versions of peptides from the same precursors and alternatively cleaved peptides that differ in the length of their N-terminal region (Supplementary file 2 and Supplementary file 3).

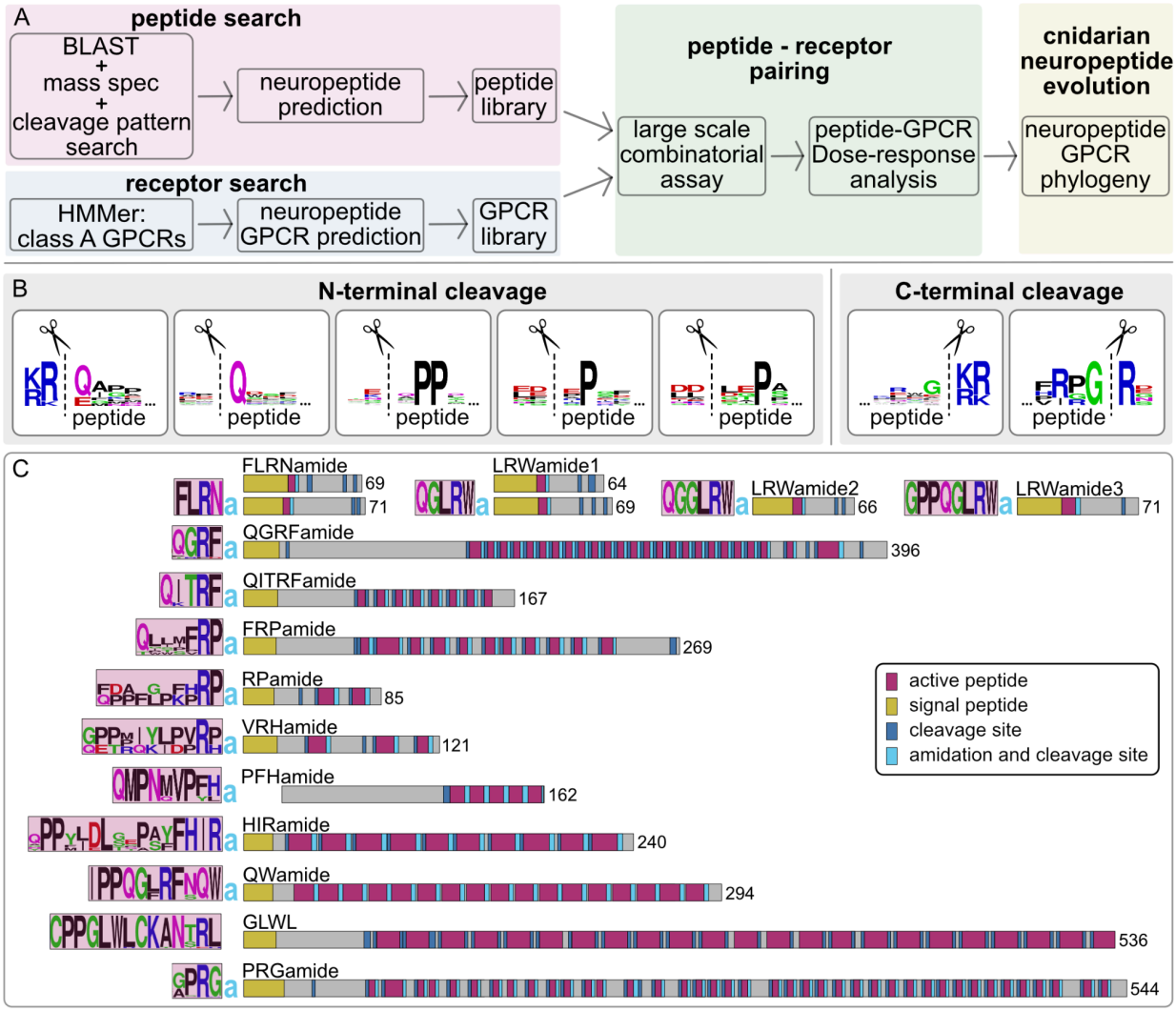

Figure 1: Identification of *Nematostella vectensis* neuropeptides. (**A**) Pipeline to identify neuropeptides and their receptors and to reconstruct the evolution of cnidarian peptidergic signaling. (**B**) Peptide sequence logos of N-terminal and C-terminal peptide cleavage sites based on peptides detected by LC-MS/MS. Cleavage occurs at the dashed lines. (**C**) *N. vectensis* neuropeptide precursor schemes of peptides for which we identified a receptor, with sequence logos of the encoded peptide(s) on the left and length of precursor on the right. a = amide.

Analysis of metazoan class A GPCRs and selection of *N. vectensis* neuropeptide-receptor candidates

To identify neuropeptide-GPCR candidates in *N. vectensis*, we focused on class A GPCRs representing the main type of neuropeptide receptors in bilaterians (Jékely, 2013; Mirabeau and Joly, 2013). We first aimed to get an overview of the diversity of class A GPCRs across metazoans and screened transcriptomes of nine cnidarian, six bilaterian, two placozoan, three ctenophore and five sponge species for these receptors (Supplementary file 5, 6). The number of GPCRs across Metazoa varies by species and seems not to correlate with phylogenetic affiliation (Figure 2A). From the combined *N. vectensis* transcriptomes (see Supplementary file 5) we initially detected a total of 1061 class A GPCR sequences. We analyzed these together with over 7000 GPCRs retrieved from the other species. As a reference, we used the experimentally confirmed and annotated human, *Drosophila melanogaster*, *Caenorhabditis elegans*, and *Platynereis dumerilii* sequences. We carried out a sequence-similarity-based clustering analysis of all sequences. This revealed only a few well-connected clusters of receptors conserved across all major metazoan lineages (Figure 2–figure supplement 1). These include the leucine-rich-repeat containing (lrrc) GPCRs, which are receptors for larger peptides such as bursicons and related glycoprotein hormones or for relaxins and related insulin-like peptides. Other well-connected GPCR clusters were more restricted to the individual phylogenetic groups. Mammalian olfactory receptors represent such a GPCR cluster with limited taxonomic breadth (Figure 2–figure supplement 1).

For a more detailed analysis, we then reduced our sampled species to cnidarians,bilaterians with experimentally confirmed GPCRs, *Petromyzon marinus*, and two placozoan species (Figure 2B). We re-ran the clustering analysis and filtered out non-connected single sequences, species-specific cnidarian clusters and unconnected clusters only containing bilaterian or placozoan sequences. The two major clusters in our GPCR map contain bilaterian and cnidarian sequences, interspersed with only a few placozoan GPCRs (Figure 2C). In both major clusters, cnidarian and bilaterian sequences form separate subclusters, rather than cnidarian GPCRs being interspersed with bilaterian GPCRs. One of these clusters contains bilaterian GPCRs for low-molecular-weight neurotransmitters, including monoamines, trace amines, acetylcholine, melatonin and ATP. This cluster is weakly connected to the opsins. The second major cluster contains most bilaterian neuropeptide receptors (Figure 2C - neuropeptide II, III, gamma) as well as the bilaterian-specific chemokine, purinergic-P2Y and fatty acid receptors. There is a second cluster of bilaterian neuropeptide receptors weakly connected to this main cluster (Figure 2C - neuropeptide I), which has only few cnidarian sequences connected to it.

Based on this cluster analysis, we selected 161 *Nematostella* GPCR sequences. We focused on full-length GPCRs that are associated with the bilaterian neuropeptide GPCR clusters. In addition, we chose candidates from non-connected clusters that are uncharacterized but ancestral to all cnidarians, except the leucine-rich repeat-containing GPCRs, which are known to be activated by insulin-related and glycoprotein-hormone-related peptides in bilaterians.

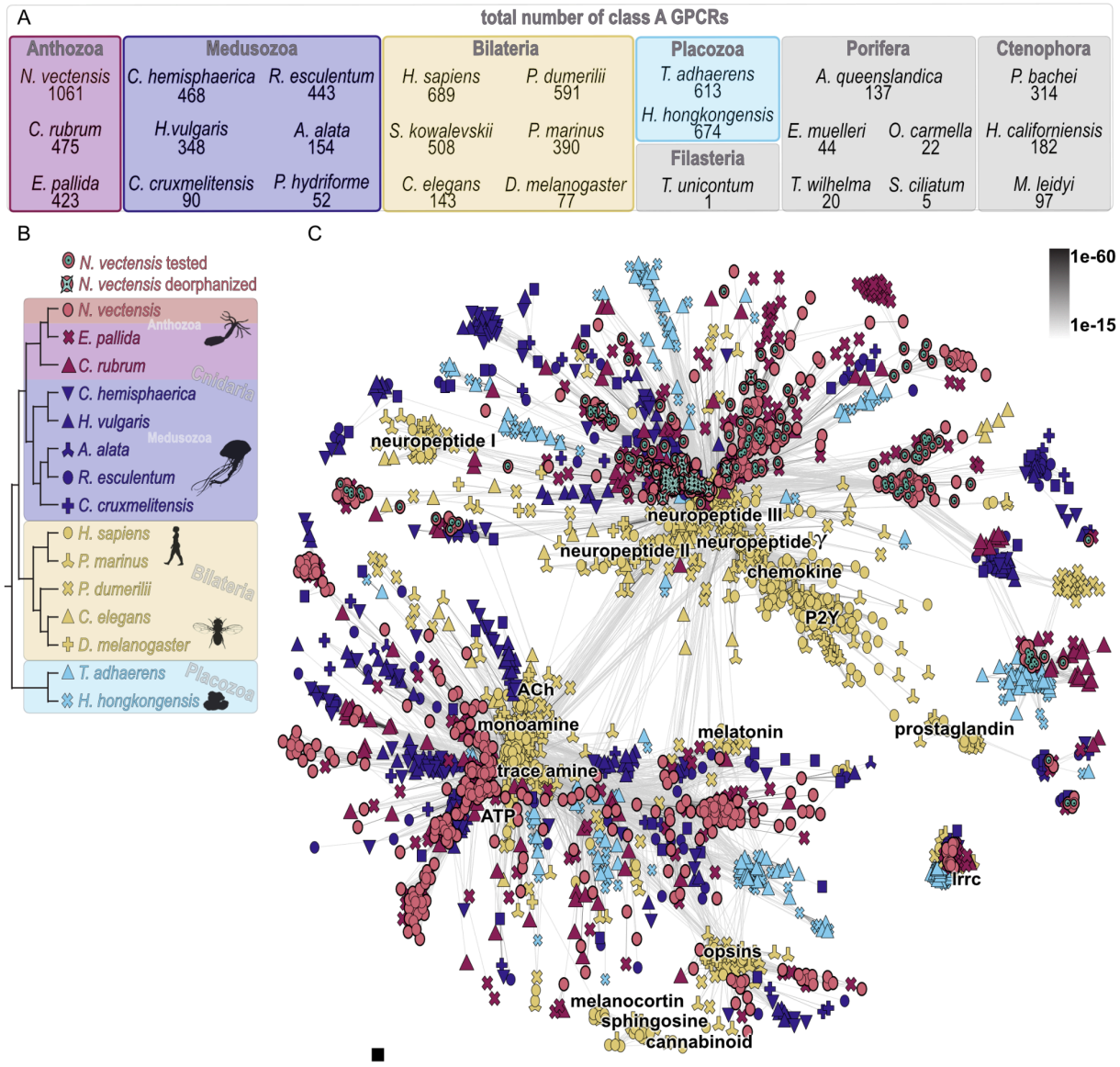

Figure 2: Cluster map of selected class A GPCRs. (**A**) Number of class A GPCRs identified by HMMer search in the different investigated species. (**B**) Relationship of species used for cluster analysis in C. (**C**) Cluster analysis of major class A GPCR groups from cnidarian, bilaterian and placozoan species. Each dot represents a GPCR sequence with color-coding and symbols according to the phylogeny in B. Connecting lines between single sequences show similarity with P-values indicated in the top right. Cluster annotations are based on

deorphanized bilaterian class A GPCRs. Abbreviations in C: ACh = acetylcholine, lrrc = leucine rich repeat containing, P2Y = purinergic P2Y receptor. Silhouette images in B were taken from phylopic.org.
Figure 2–source data 1. Raw cluster analysis CLANS file.

Deorphanization of 31 *Nematostella* neuropeptide receptors

To experimentally identify *Nematostella* neuropeptide GPCRs, we tested our selection of 161 *N. vectensis* GPCRs in a pharmacological assay for activation by peptides from our peptide library (Figure 3A, Supplementary file 3, 8). We expressed the candidate GPCRs in mammalian cells, together with a promiscuous Gqi protein and a luminescent G5A reporter (Figure 3A, Supplementary file 7). The peptides were separated into different mixes (Supplementary file 3), which were then tested on each GPCR (Supplementary file 4). Receptor-mix combinations that gave a positive signal were further resolved by testing the individual peptides of the mix to identify the activating ligand (Supplementary file 4). Peptides activating a receptor were then tested at different concentrations to record dose-response curves and determine EC_{50} values for each peptide-receptor pair (Supplementary file 9).
In this screen, we identified 31 *N. vectensis* GPCRs activated mostly in the nanomolar range by peptides from 14 different precursors (Figure 1C, 3B, C, D; Supplementary file 10). The neuropeptides GLWL, PFHamide, VRHamide and QWamide each activate a different, single receptor (GLWL/R18 EC_{50} = 9E-7, PFHa/R36 EC_{50} = 1.2E-8, VRHa/R186 EC_{50} = 2.7E-10, QWa/R69 EC_{50} = 9E-7). Peptides ending in RPamide from the HRPamide and FRPamide precursors activate the same, single receptor R248. The HRPa peptide has a lower EC_{50} value, the FRPa peptide, however, has a lower threshold activation while reaching its maximum activation at higher concentrations with an overall more shallow curve slope (HRPa/R248 EC_{50} = 8.9E-9, HRPa/R248 slope = 1.75, FRPa/R248 EC_{50} = 2.3E-7, FRPa/R248 slope = 0.42) (Supplementary file 10).
The RFamide peptides with the sequence pyrQGRFamide and pyrQITRFamide are each encoded on separate precursors and despite their strong sequence similarities each activate separate receptors (pyrQGRFa/R70 EC_{50} = 2.1E-6, pyrQGRFa/R234 EC_{50} = 4.7E-9, pyrQITRFa/R196 EC_{50} = 7.7E-11) although one of the two pyrQGRFamide receptors is also activated by higher concentrations of pyrQITRFamide (QITRFa/R70 EC_{50} = 1.7E-5). Given that R70 has EC_{50} values in a lower micromolar range for both RFamides, it is possible that this receptor has another unknown ligand that is more specific but shares some structural similarity to these RFamides.
Two receptors are activated by HIRamide (R21 EC_{50} = 2.1E-9, R29 EC_{50} = 1.9E-7). The more sensitive R21, however, showed a strong base-activation at all tested concentrations, leading to a shifted EC_{50} for which we adjusted the minimum values (Figure 3–figure supplement 1). We also tested different copy versions of HIRamide peptides and most activated the two receptors in a similar concentration range (Figure 3–figure supplement 1).
Four receptors are activated by FLRNamide (FLRNa/R26 EC_{50} = 7.4E-8, FLRNa/R187 EC_{50} = 7E-8, FLRNa/R197 EC_{50} = 1.1E-8, FLRNa/R230 EC_{50} = 4.7E-9), and one of these is also sensitive to higher concentrations of FYRVamide (FYRVa/R197 EC_{50} = 1.1E-6). However, we

only tested the non-modified FLRNamide peptide and not the phenylacetyl-LRNamide as described to exist in sea anemones (Grimmelikhuijzen et al., 1990) which may be a better ligand.

The three LRWamide peptides pyrQGLRWamide (LRWa1), pyrQGGLRWamide (LRWa2) and GPPQGLRWamide (LRWa3), which are each encoded as a single copy on separate precursors (Figure 1C), cross-activate 4 different GPCRs. Each LRWamide seems to have one preferred receptor (LRWa1/R19 EC_{50} = 9.1E-8, LRWa2/R213 EC_{50} = 3.1E-8, LRWa3/R204 EC_{50} = 7.4E-10) plus a fourth GPCR (R193) which appears similarly sensitive to all LRWamide peptides (LRWa1/R193 EC_{50} = 6.6E-11, LRWa2/R193 EC_{50} = 2E-10, LRWa3/R193 EC_{50} = 6.9E-10). Receptor 19 and 204 have clearly shifted curves and lower EC_{50} values for their preferred peptide, while Receptor 213 has similar EC_{50} values for LRWa1 (EC_{50} = 5.4E-8) and LRWa2 (EC_{50} = 3.1E-8) but is more sensitive to LRWa2 at lower concentrations while reaching its maximum activation later.

Finally, the PRGamide peptide, which belongs to the ancestral cnidarian PRXamides, activates at least 13 different receptors (R28, R32, R198, R199, R200, R202, R210, R211, R219, R220, R221, R222, R223) in *Nematostella* with EC_{50} values between 1.6E-10 and 4.5E-8. We also tested R28 and R32 with longer versions of the PRGamide, as these were described elsewhere based on mass spectrometry data (Hayakawa et al., 2019). The higher EC_{50} values for these longer PRGamides (Figure 3–figure supplement 2) and the sequences on the precursor themselves (Supplementary file 2), however, suggest that these are not fully processed and the actual PRGamide is a tetrapeptide (GPRGamide and APRGamide) as previously suggested (Koch and Grimmelikhuijzen, 2020). The same is likely true for the longer QGRFamide version (QGRFGREDQGRFamide) (Hayakawa et al., 2019) which is also likely not fully processed as in this case the activation of the QGRFamide receptors in the initial screen was much lower for the mix that contained the longer version than for the mix containing the fully processed pyrQGRFamide peptide (Supplementary file 4 - mix 4 vs. mix 6).

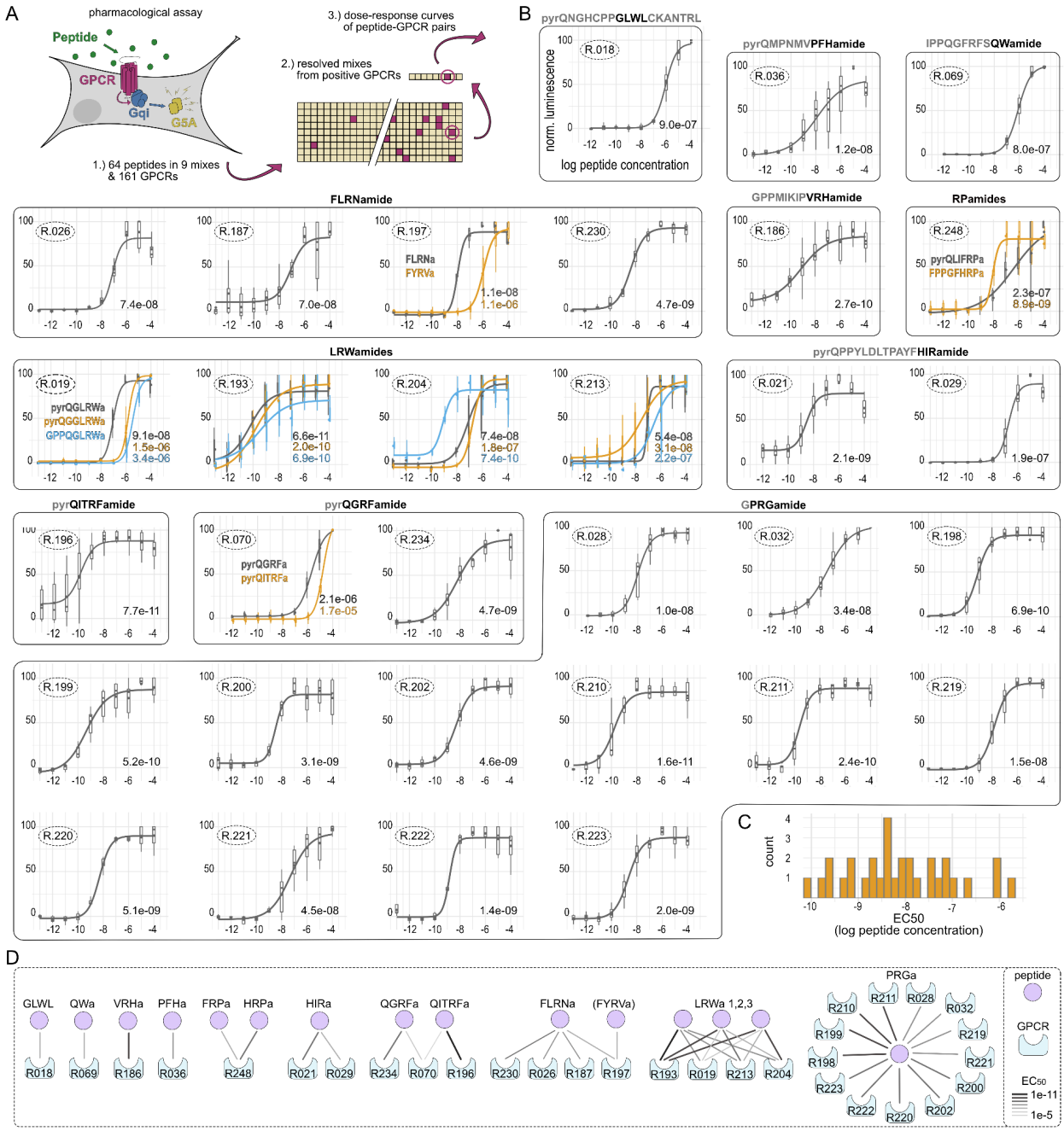

Figure 3: Dose-response curves of *Nematostella* neuropeptide GPCR pairs. (**A**) Pharmacological assay and pipeline to identify peptide-GPCR pairs. (**B**) Dose-response curves of peptide-GPCR pairs with log peptide concentration plotted against normalized luminescence. GPCRs that are activated by the same peptide(s) are grouped together with peptide sequence shown above and peptide name highlighted in black. If several peptides activate the same receptor, peptide sequences are shown within the graph. Receptor identification number is encircled in the upper left of each curve, EC_{50} values are indicated in the lower right. (**C**) Histogram of EC_{50} values of peptide-GPCR pairs, showing only the lowest EC_{50} per GPCR. (**D**) Peptide-receptor pairings showing number of receptors activated by the different peptides. Connection strength indicates EC_{50} values.

Figure 3–source data 1. Tibble with all data points used to calculate the dose-response curves and EC_{50} values, in .csv format.

At least nine neuropeptide GPCR families are ancestral to cnidarians

To reconstruct the evolution of neuropeptide receptors in animals, we analyzed the phylogenetic relationships of the 31 deorphanized *N. vectensis* neuropeptide GPCRs to other cnidarian and bilaterian GPCRs. From the clustermap (Figure 2), we chose sequences with connection to the bilaterian and cnidarian neuropeptide GPCR clusters and calculated phylogenetic trees. In an initial analysis, we found that the bilaterian chemokine, purino, fatty acid and other related bilaterian-specific receptors are likely a diverged ingroup of the bilaterian neuropeptide gamma rhodopsin receptors (Figure 4–figure supplement 1,2, Supplementary file 11). Gamma rhodopsin receptors are specific to bilaterians and include somatostatin/allatostatin A, opioid/somatostatin/allatostatin C, kisspeptin and melanin-concentrating hormone receptors (Mirabeau and Joly, 2013; Thiel et al., 2021). We then deleted redundant group-specific expansions of loosely connected orphan clusters, the non-neuropeptide chemokine and related receptors, decreased the number of bilaterian species and calculated a detailed neuropeptide-GPCR phylogeny (Figure 4, Supplementary file 11).

The majority of known neuropeptide GPCRs are grouped into three main bilaterian clusters and two main cnidarian clusters (Figure 4B). Within the two cnidarian clusters, there are at least nine neuropeptide GPCR families that are ancestral to Cnidaria, all of which are represented with clear anthozoan and medusozoan orthology groups. The deorphanized *N. vectensis* neuropeptide GPCRs belong to at least seven of these ancestral cnidarian families (Figure 4B, C).

One of the two main cnidarian clusters seems to have only expanded late within the Hexacorallia branch, with an especially high number of more than 100 GPCRs in *N. vectensis* (Figure 4B,C). The entire cluster is expanded in *N. vectensis* and *Exaiptasia pallida*, but neither expanded in *Corallium rubrum*, nor in medusozoan species. This cluster likely expanded from a single ancestral cnidarian receptor family as it only contains a single branch of medusozoan sequences. Alternatively, this cluster can be traced back to two peptidergic systems, with a loss of medusozoan sequences in one of them. This cluster contains the more promiscuous and less sensitive *N. vectensis* QGRFamide GPR70, the QWamide GPR69 and the PFHamide GPR36.

The second major cnidarian neuropeptide GPCR cluster contains at least eight ancestral cnidarian receptor families, based on the presence of clear anthozoan and medusozoan orthology groups, with deorphanized *N. vectensis* receptors in six of them (Figure 4B,C). The QITRFamide GPR196 belongs to a small group of hexacorallian receptors with no clear orthologs in *C. rubrum* or any medusozoan species, which might either represent a separate ancestral group with no medusozoan representative sequences or a strongly diverged Hexacorallia subcluster. This is in accordance with the absence of QITRFamide peptides in Octocorallia and Medusozoa (Koch and Grimmelikhuijzen, 2020). The QGRFamide GPR234 belongs to an ancestral cnidarian GPCR family, which is in accordance with the existence of QGRFamide or GRFamide peptide precursors across Cnidaria (Koch and Grimmelikhuijzen,

2020, 2019). This group is slightly expanded in the medusozoans *Clytia hemisphaerica* and *Hydra vulgaris*. The entire QGRFamide family seems related to the LRWa GPR19 containing group, which has otherwise no direct orthologous sequences in medusozoans. The GLWL peptide receptor GPR18 belongs to an ancestral cnidarian family that shows a slight expansion in *N. vectensis*. The receptors for the peptides LRWamide, FLRNamide and HIRamide are closely related as part of an anthozoan/hexacorallian expansion, curiously twice in unrelated families. Each of the families is ancestral to cnidarians and one expanded in anthozoans and additionally contains the receptors for VRHamide and RPamides, while the other group only showed several sequences in the two analyzed Hexacorallia species *N. vectensis* and *E. pallida*. Both families contain receptors for the three peptides, LRWamide, FLRNamide and HIRamide, and both families only contain medusozoan sequences from *R. esculentum* and *C. cruxmelitensis*. The 13 PRGamide receptors of *N. vectensis* belong to two separate ancestral cnidarian families, both of which are expanded in anthozoans. One PRGamide family independently also expanded in *Hydra vulgaris*. The other PRGamide family contains the *Clytia* MIH receptor which is activated by *Clytia* PRXamides (Artigas et al., 2020), confirming a peptide-receptor coevolution in cnidarians for the ancestral PRXamides (Koch and Grimmelikhuijzen, 2019) and their receptor(s).

Cnidarian and bilaterian neuropeptide GPCR systems expanded after the cnidarian-bilaterian split from a few ancestral systems

Our phylogenetic analyses divided the cnidarian and the bilaterian neuropeptide receptors into very few major clusters, each containing either bilaterian or cnidarian sequences (Figure 4B). The relationship of these major clusters to each other is not well resolved. However, the general clustering (Figure 2C) in combination with the phylogenetic analysis (Figure 4B) shows that these groups represent many-to-many bilaterian-cnidarian orthology groups. Most of the bilaterian and cnidarian class-A neuropeptide GPCRs therefore diversified after the bilaterian-cnidarian split. The only family with an apparently consistent one-to-one orthology of an ancestral cnidarian and bilaterian branch of receptors is that of the bilaterian orphan receptor GPR19.

In addition there are a few branches with unclear phylogeny or restricted taxonomic breadth. A small group of anthozoan orphan receptors without medusozoan representatives shows affinity to the expanded cluster of bilaterian oxytocin/vasopressin, GnRH, achatin and neuropeptide S/CCAP receptors, suggesting a one-to-many orthology. This affinity is consistent in different trees (compare Figure 4 and Figure 4–figure supplement 1,2, or Supplementary file 11). Other orthology groups between Cnidaria and Bilateria are less clear and the potential branches in question are not stable between the different phylogenies. The bilaterian SIFamide GPCR grouped together with an orphan cnidarian branch, but varied in its position in other analyses (compare Figure 4 and Figure 4–figure supplement 1 and 2, or Supplementary file 11). This instability is also obvious due to the fact that the SIFamide GPCR is the protostome ortholog of the deuterostome NpFF GPCRs, which would have been expected to group together. Accordingly, the NpFF receptor was also unstable in our analyses. The NpFF and SIFamide receptor group is usually well supported, but often shows long basal branches and these two

together built in previous analyses a more separated branch with unstable relationship to other bilaterian receptor groups (Mirabeau and Joly, 2013; Thiel et al., 2021, 2018). The bilaterian QRFPR branch has a likewise unstable relationship to other bilaterian neuropeptide GPCRs in previous analyses but showed affinity to the SIFamide/NpFF GPCRs in some analyses (Jékely, 2013; Thiel et al., 2018). Accordingly, the affinity of some *N. vectensis* sequences to the QRFPR branch is also not stable in our different analyses (compare Figure 4 and Figure 4–figure supplement 1 and 2; Supplementary file 11). Two ancestral cnidarian branches grouped together with the *Drosophila* trissin receptor, but also this is an unstable grouping not present in our supplementary analyses (Figure 4–figure supplement 1 and 2). The trissin receptor is a generally peculiar bilaterian protostome receptor as no orthologous deuterostome sequences are known (Elphick et al., 2018; Mirabeau and Joly, 2013; Thiel et al., 2021). The orexin/allatotropin receptors showed no direct orthology to cnidarian receptors, but appear as a sister group to a branch with orphan bilaterian and placozoan GPCRs. Together, except for the GPR19 group, we could not find cnidarian receptors that show a consistent 1:1 orthology relationship to specific bilaterian receptors such as for example proposed for orexin/allatotropin, somatostatin, neuropeptide Y or tachykinin receptors (Alzugaray et al., 2019; Anctil, 2009; Krishnan and Schiöth, 2015). This is in accordance with other analyses that used a wider array of bilaterian neuropeptide GPCRs when comparing them to cnidarian GPCR sequences (Artigas et al., 2020; Hauser et al., 2022; Thiel et al., 2018) and found rather many-to-many orthologs, if any at all.

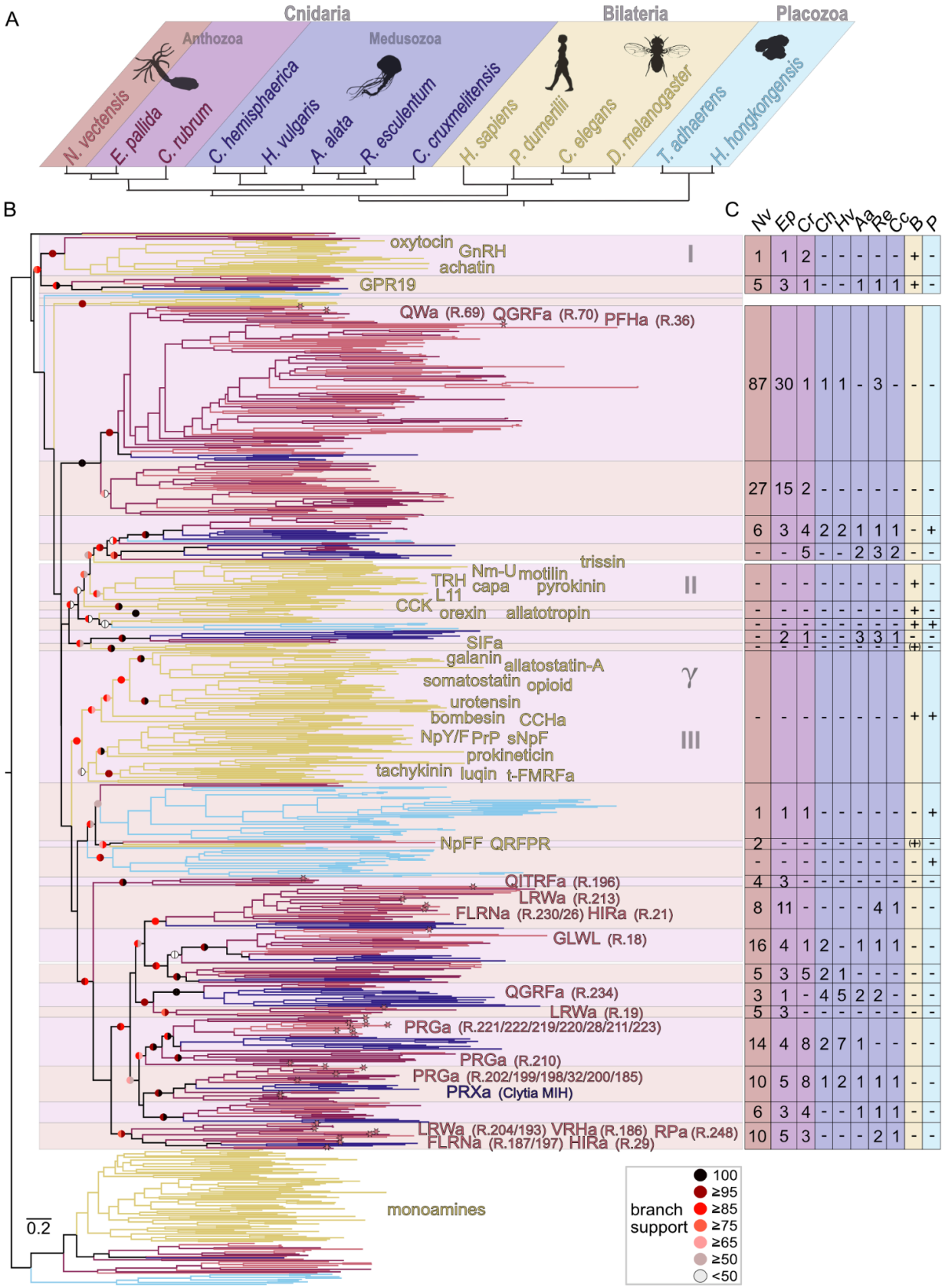
A
Cnidaria
Bilateria
Placozoa
Anthozoa
Medusozoa
N. vectensis
E. pallida
C. rubrum
C. hemisphaerica
H. vulgaris
A. alata
R. esculentum
C. cruxmelitensis
H. sapiens
P. dumerilii
C. elegans
D. melanogaster
T. adhaerens
H. hongkongensis
B
C
Nv Ep Cr Ch Hv Aa Re Cc B P
oxytocin GnRH achatin
GPR19
QWa (R.69) QGRFa (R.70) PFHa (R.36)
trissin
Nm-U motilin
TRH capa pyrokinin
L11
CCK orexin allatotropin
SIFa
galanin allatostatin-A
somatostatin opioid
urotensin
bombesin CCHa
NpY/F PrP sNpF
prokineticin
tachykinin luqin t-FMRFa
NpFF QRFPR
QITRFa (R.196)
LRWa (R.213)
FLRNa (R.230/26) HIRa (R.21)
GLWL (R.18)
QGRFa (R.234)
LRWa (R.19)
PRGa (R.221/222/219/220/28/211/223)
PRGa (R.210)
PRGa (R.202/199/198/32/200/185)
PRXa (Clytia MIH)
LRWa (R.204/193) VRHa (R.186) RPa (R.248)
FLRNa (R.187/197) HIRa (R.29)
monoamines
I
II
γ
III
0.2
branch support
100
≥95
≥85
≥75
≥65
≥50
<50

Figure 4: Phylogeny of metazoan class A neuropeptide GPCRs. (**A**) Phylogeny of species used in B. (**B**) Phylogeny of neuropeptide GPCRs with names of ligands. Branches are color coded according to A. Branches of deorphanized *Nematostella* GPCRs end in an asterisk. Alternating shades behind the tree branches highlight different monophyletic groups. Roman Numbers 1-3 and greek symbol gamma indicate approximate neuropeptide clusters shown in Figure 2. Left half circle of branch support indicates aBayes and the right half circle aLRT-SH-like support values. Detailed annotations in Supplementary file 11. (**C**) Table with number of receptors per group as highlighted in receptor phylogeny with a straight line indicating no receptor present. Two-letter abbreviations on top correspond to species in A. Abbreviations: a = amide, B = Bilateria, CCK = cholecystokinin, GnRH = gonadotropin releasing hormone, MIH = maturation-inducing hormone, Nm-U = neuromedin U, NpFF = neuropeptide FF, NpY/F = neuropeptide Y/neuropeptide F, P = Placozoa, PrP = prolactin releasing peptide, R.# = *Nematostella* GPCR number, sNpF = short neuropeptide F, t-FMRFa = trochozoan FMRFamide, TRH = thyrotropin releasing hormone.
Figure 4–source data 1. Raw sequences used for tree building, .fasta format.
Figure 4–source data 2. Aligned sequences used for tree building.
Figure 4–source data 3. Trimmed sequence alignment used for tree building.
Figure 4–source data 4. Tree file in nexus format.

Cell-type-specific expression of neuropeptides and GPCRs and the peptidergic connectome of *Nematostella*

To analyze tissue-level peptidergic signaling in *N. vectensis*, we mapped the expression of neuropeptide precursors and the newly deorphanized neuropeptide GPCRs to a single-cell RNAseq dataset (Cole et al., 2024; Steger et al., 2022). The single-cell data are split into two sets, one consisting of pooled stages spanning 18 hours post-fertilization to 16-day-old primary polyp (developmental set) and the second set consisting of adult tissues only, similar to (Cole et al., 2024, 2023). The expression of GPCRs was in many cases low and only a small percentage of cells within a given cell cluster show receptor expression. We could not detect expression of GLWL receptor R18 and HIRamide receptor R29, consistent with the generally low expression of GPCRs in animals (Fredriksson and Schiöth, 2005; Regard et al., 2008; Soave et al., 2021; Sriram et al., 2019). In contrast, neuropeptide precursors are generally highly expressed in neurons (Smith et al., 2019) and we could detect all of them, except for the PFHamide that could not be mapped and was only present as a partial sequence in our combined transcriptome (Figure 1C). Most neuropeptide precursors show restricted expression in neuroglandular cells (Figure 5B), with the exception of the phoenixin and GLWL precursors (Figure 5–figure supplement 1). The broad expression of phoenixin suggests other functions for this molecule outside neuronal signaling, for example in mitochondrial regulation (Dennerlein et al., 2015; Yañez-Guerra et al., 2022).
Individual GPCRs were often restricted to a single or very few tissue types (Figure 5B for tissue type overview and Supplementary file 12 for cell-type-specific resolution). For peptides with multiple receptors, we often found distinct patterns of receptor expression. Individual PRGamide receptors are for example restricted to the retractor muscle (R221, R222), the gastrodermis (R211), embryonic putative stem cells (pSC) (R210) or a combination of neuroglandular cells and adult cnidocytes (R202) (Figure 5B). An exception is the PRGamide receptor R200, which

shows expression in a wide array of tissues, including adult pSC, primary germ cells (PGCs), neuronal cells, immune cells, and embryonic ectodermal cells.

The different LRWamide receptors also signal to different tissue types. The receptor R204, which is most sensitive to LRWa3, is strongest expressed in embryonic endomesodermal cells and the pharyngeal ectoderm, the receptor R19, which is most sensitive to LRWa1 is found in neuroglandular cells, the receptor R213, which showed highest sensitivity to LRWa2 is found in neuroglandular and glandular mucousal cells and the receptor R193, which is similarly sensitive to all LRWamides is only present in glandular mucousal cells. The two receptors of the ancestral QGRFamide are also differentially expressed, with the receptor R70 only present in adult neuroglandular cells, while the highly specific R234 is additionally expressed in developmental and adult glandular mucousal cells and in some developmental retractor muscle cells.

Within the neuroglandular subset, each neuronal cell type expresses a unique combination of neuropeptide precursors and GPCRs (Figure 5–figure supplement 2 and 3; Supplementary file 12). Most peptide precursors are thereby restricted to only a few cell types. PRGamide for example, is restricted to two types of neuroglandular cells: the larval apical organ N1.L2 cells and the N2.g1 cells, which persist in adults (Figure 5–figure supplement 2,3). This restricted expression of the PRGamide precursor is also in accordance with previously published in situ hybridizations that show a restricted expression in the larval apical organ (Gilbert et al., 2022). Many neuronal cell types only express a low number of different neuropeptide precursors, with few exceptions such as the mentioned N1.L2 cells or the N1.L3 and N1.4 cells, which express between 4-8 different types of neuropeptide precursors, depending on the stage. The larval N1.L2 cells express the PRGamide, VRHamide, QITRFamide, RPamide, LRE peptide, GLWL peptide and the phoenixin precursor, while only expressing two receptors: the PRGamide receptor R.200 with a lower average expression and the VRHamide receptor R186. The expression of both the PRGamide and VRHamide peptide precursors and receptors may indicate autocrine regulation in these cells. The second PRGamide-positive cell type N2.g1 that persists in adults, also shows in both datasets an expression of the PRGamide precursors and a different PRGamide receptor R.221, which is only found in few cell types and similarly may mediate autocrine feedback.

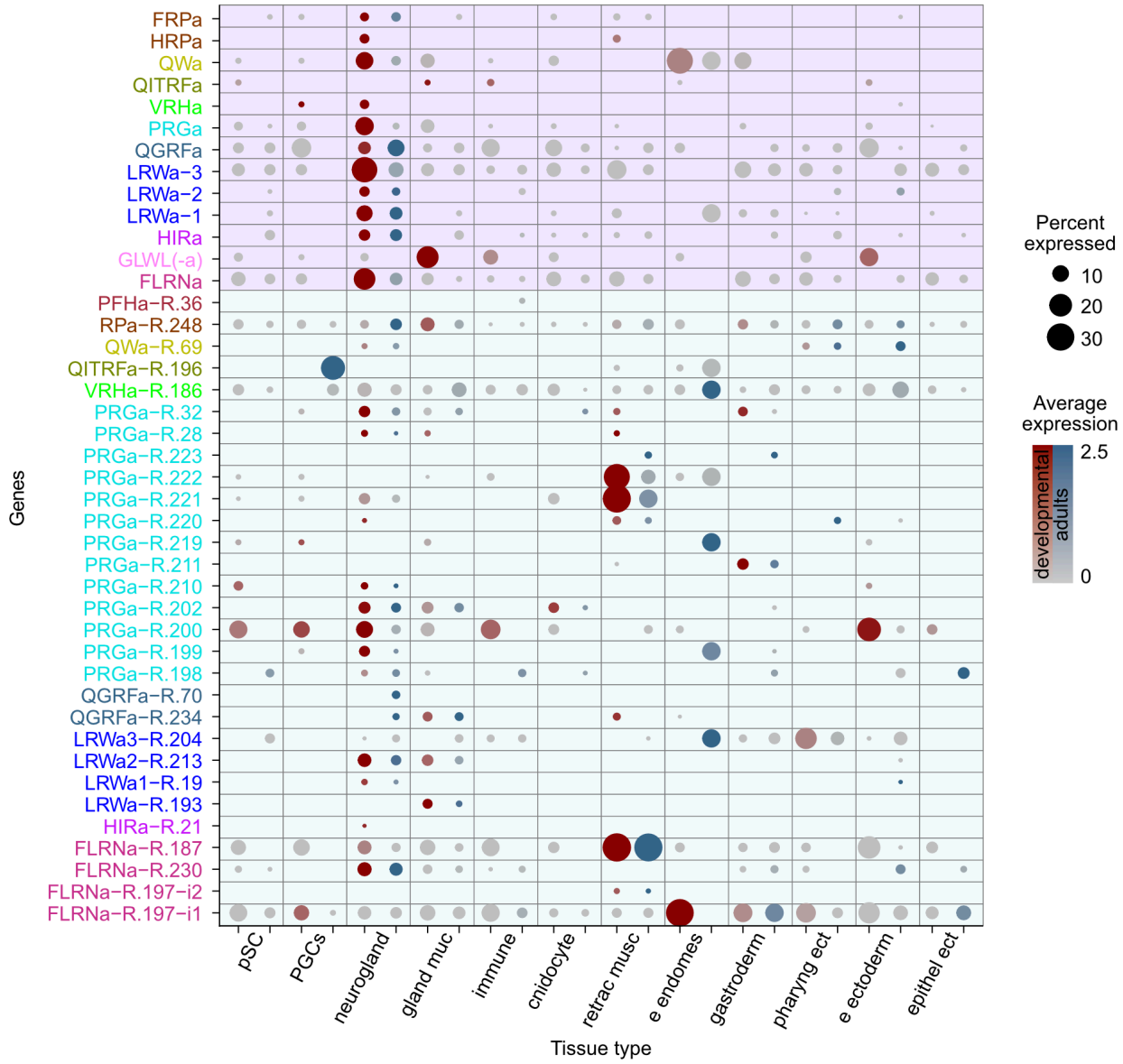

Figure 5: Tissue-specific expression of neuropeptide precursors and receptors (GPCRs) in *N. vectensis*. Dotplot for tissue-specific expression of peptide precursors and GPCRs. Red dots indicate expression in the developmental dataset, blue dots indicate expression in the adult dataset. Abbreviations: a = amide, e = embryonic, ect = ectoderm, endomes = endomesoderm, gland = glandular, muc = mucous, musc = muscle, neurogland = neuroglandular, PGC = primary germ cells, pharyng = pharyngeal, pSC = putative stem cells, R = receptor (GPCR), retrac = retractor.

To determine the global organization of peptidergic signaling networks or the 'peptidergic connectome' (Bentley et al., 2016; Deng et al., 2019; Smith et al., 2019; Williams et al., 2017) in *Nematostella*, we constructed a multi-layered network for both the developmental and the adult dataset (Figure 6, Figure 6–figure supplement 1). In these networks, nodes represent cell/tissue types and links are defined from peptide-expressing cells to receptor-expressing cells taking into account expression levels and the EC_{50} values. Different peptide-receptor pairs (represented by

different colors in Figure 6, Figure 6–figure supplement 1 B-D, F-L) form distinct layers in this multi-layer connectome. By modularity analysis, we subdivided the networks into three (developmental) or four (adult) modules, each dominated by peptides with multiple receptors: PRGamide, pyrQGRFamide, FLRNamide and LRWamide (Figure 6–figure supplement 1 A,E). The cells at the center of these modules that are most strongly involved in peptidergic signaling are the N1.g3, N1S.3, N1.L2, N1.L3, and N2.g1 cells in the developmental dataset and the N1.g3, N1S.3, N1.g2 and N2.g1 cells in the adult dataset.

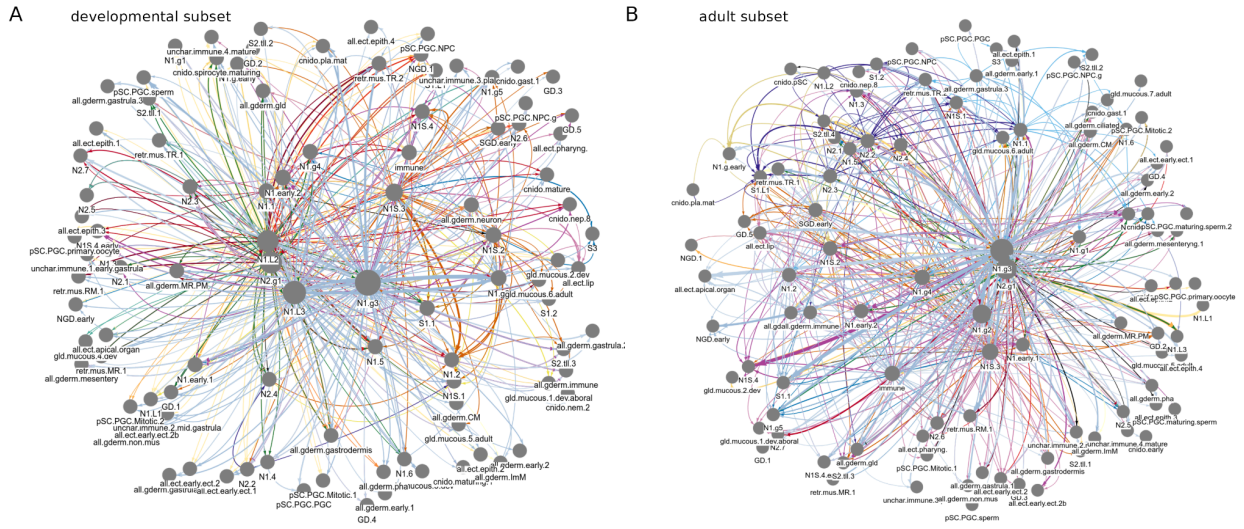

Figure 6: Multi-layer peptidergic connectomes in *Nematostella.* Peptidergic networks in the (**A**) developmental and (**B**) adult subset**.** Nodes represent cell types, connections represent potential peptidergic signaling from neuropeptide-expressing cells to cells expressing one or more of the receptors for that neuropeptide. Colors represent different peptide-receptor signal channels (the different layers in the multi-layer connectome).
Figure6–source data 1. Graph file of the multilayered peptidergic connectome in the developmental subset. A serialized binary file in tbl_graph format, to be analyzed in R.
Figure6–source data 2. Graph file of the multilayered peptidergic connectome in the developmental subset. In Gephi .gexf format, to be analyzed in Gephi.
Figure 6–source data 3. Graph file of the multilayered peptidergic connectome in the adult subset. A serialized binary file in tbl_graph format, to be analyzed in R.
Figure 6–source data 4. Graph file of the multilayered peptidergic connectome in the adult subset. In Gephi .gexf format, to be analyzed in Gephi.

Discussion

We deorphanized 31 neuropeptide GPCRs of the sea anemone *Nematostella vectensis* and reconstructed their evolution and relationship to other cnidarian orphan GPCRs and bilaterian neuropeptide GPCRs. Our phylogeny suggests that the identified neuropeptide GPCRs belong to two major GPCR clades that expanded independently of each other. One clade diversified in stem Cnidaria into eight receptor families that are all present across medusozoans and anthozoans. The other clade diversified later within the anthozoans, likely from a single ancestral cnidarian receptor. The expansion of GPCR systems is a general feature of GPCR evolution and happened independently in different lineages and at different times during animal evolution (Beets et al., 2022; Mirabeau and Joly, 2013).

The cnidarian neuropeptide receptors we identified here show many-to-many orthology relationship to bilaterian neuropeptide GPCRs. We did not identify any direct receptor orthologs between cnidarians and bilaterians, indicating extensive parallel expansion of neuropeptide signaling in the two clades. Previously, some neuropeptides have been hypothesized to be orthologous across cnidarians and bilaterians, including neuropeptides ending in an RFamide (Jékely, 2013; Walker et al., 2009), which is a frequent motif (Elphick and Mirabeau, 2014; Jékely, 2013; Walker et al., 2009). We identified two *N. vectensis* RFamide receptors, one for the ancestral cnidarian neuropeptide pyrQGRFamide (Koch et al., 2021; Koch and Grimmelikhuijzen, 2019) and one for the hexacorallia pyrQITRFamide. These two *N. vectensis* receptors belong to either of the two major clades of cnidarian receptors, suggesting that new RFamide receptors and/or peptides can evolve independently. Likewise, within bilaterians there are many RFamides across protostomes and deuterostomes that are not orthologous to each other (Elphick and Mirabeau, 2014; Thiel et al., 2021). The cnidarian RFamide receptors are also more closely related to other cnidarian neuropeptide receptors than to bilaterian RFamide receptors, arguing against the orthology of cnidarian and bilaterian RFamides. C-terminal aromatic amino acids are found in various neuropeptides and also many monoamine receptors are activated by derivatives of aromatic amino acids (Bauknecht and Jékely, 2017; Elphick and Mirabeau, 2014). Aromatic amino acids might have been early ligands in the evolution of monoamine neurotransmission and ancestrally present as a common structural feature at the C-termini of neuropeptides activating peptide receptors.

Our phylogenetic analyses and GPCR resource will be useful to directly predict the ligand of neuropeptide receptors in other cnidarian species. We expect this because of the long-term coevolution of peptide-receptor pairs that has been extensively documented in bilaterians. The orthology of six of the identified anthozoan *N. vectensis* PRGamide receptors to the PRXamide receptor of the hydrozoan *C. hemisphaerica* is the first example of a similar long-term ligand-receptor association across cnidarians. Receptors of ancient peptides such as PRXamides or GRFamide are therefore expected to be orthologous even in distantly related cnidarians. Other Hexacorallia- or Anthozoa-specific peptides such as HIRamide, FLRNamide and LRWamide (Koch and Grimmelikhuijzen, 2020) can be tested on directly orthologous receptors. Phylogenetic analyses combined with targeted deorphanization experiments of predicted orthologs could thus lead to the rapid characterisation of new receptors in other cnidarians.

Our large-scale GPCR-peptide resource also allowed us to analyze tissue-level peptidergic networks in *N. vectensis*. With high-resolution single-cell resources becoming available in a larger number of species, it will be possible to predict the cellular targets of neuropeptide signals with increasing precision based on receptor expression. The unique combinations of proneuropeptides and neuropeptide receptors in the different neuronal cell types can also be used as markers to identify and characterize neuronal cell types. The uniquely specific combinatorial expression of proneuropeptides as neuronal markers parallels the situation found in bilaterian nervous systems, where proneuropeptides provide fingerprint-like identities to different neuronal cell types (Smith et al., 2019; Taylor et al., 2021; Williams et al., 2017).
Finally, our work also opens up new avenues in experimental neuroscience in cnidarians (Bosch et al., 2017). With readily available genetic manipulation techniques in *N. vectensis* and other species (Ikmi et al., 2014; Nakanishi and Martindale, 2018; Paix et al., 2023)(Artigas et al., 2020; Sanders et al., 2018; Wittlieb et al., 2006), the identified neuropeptide-receptor interactions will enable genetic manipulations of both ligand and receptor(s), to reveal the biological functions of peptidergic signaling.
Overall, we identified receptors for peptides from nearly half of the *Nematostella* neuropeptide precursors, including the receptors of the ancient PRXamide and pyrQGRFamide peptides. Future studies aiming at finding the remaining receptors could focus on GPCRs with no sequence similarity to known bilaterian neuropeptide GPCRs, including monoamine-related or leucine-rich-repeat receptors, or other types of receptors like DEG/ENaC-related ion channels (Gründer et al., 2022; Mirabeau and Joly, 2013).

Acknowledgements

We would like to thank Dr Cameron Hird for help with animal husbandry. We also thank Dr Francesca Carlisle for testing our cells for mycoplasma contamination. This work was funded by the Wellcome Trust (214337/Z/18/Z), the Leverhulme Trust (Project Grant RPG-2018-392), a BBSRC Discovery fellowship to LAYG (BB/W010305/1) and the KU Leuven grant C16/19/003.

Material and Methods

Transcriptomic resources

We collected transcriptomes and protein predictions from different metazoans (Cnidaria: *Nematostella vectensis*, *Alatina alata, Calvadosia cruxmelitensis, Clytia hemisphaerica, Corallium rubrum, Exaiptasia pallida, Hydra vulgaris, Polypodium hydriforme, Rhopilema esculentum.* Bilateria: *Drosophila melanogaster, Caenorhabditis elegans, Homo sapiens, Petromyzon marinus, Platynereis dumerilii, Saccoglossus kowalevskii.* Placozoa: *Hoilunga hongkongensis, Trichoplax adhaerens.* Porifera: *Amphimedon queenslandica, Ephydatia muelleri, Oscarella carmella, Sycon ciliatum, Tethya wilhelma,* Ctenophora: *Pleurobrachia*

bachei, Mnemiopsis leydi, Hormiphora californiensis) and the filasterian *Tunicaraptor unikontum*. Transcriptomic databases were translated to protein sequences using the tool TransDecoder (http://transdecoder.github.io/) with a minimum length of 60 amino acids. For completeness assessment of the transcriptomes, we ran BUSCO v5.2.1 in protein mode and with the lineage database 'eukaryota_odb10' (database creation: September 2022; number of BUSCOs: 255). The source of the databases used for this analysis and the results of the completeness analysis are available in Supplementary file 5. Different transcriptomes of *N. vectensis* (http://metazoa.ensembl.org/species.html, https://hdl.handle.net/1912/5613, https://simrbase.stowers.org/starletseaanemone) were translated into protein sequences and merged, followed by the use of CD-hit (Fu et al., 2012; Li and Godzik, 2006) with a similarity setting of 0.85.

Neuropeptide precursor search

Neuropeptide precursors of *N. vectensis* were identified with different bioinformatic strategies. First, we carried out BlastP analyses based on previously published datasets (Hayakawa et al., 2019; Koch and Grimmelikhuijzen, 2020; Thiel et al., 2021; Yañez-Guerra et al., 2022). Sequences with e-values < 1e-02 were manually scanned for the presence of multiple cleavage sites and similarity to known proneuropeptides. Additionally, we obtained a predicted secretome by using SignalP4.1 with the sensitive option (D-cutoff 0.34). This secretome was then used to search for novel precursors by two different methodologies. Pattern searches were done as described before (Thiel et al., 2021), based on repetitive cleavage sites. The resulting sequences were then manually checked for occurrence of similar motifs between these cleavage sites. The obtained secretome was also scanned with the machine-learning algorithm NeuroPID that enriched the number of single-copy neuropeptide precursors (Ofer and Linial, 2014). This last methodology, however, produced a large database that included thousands of hits, with a high level of false positive proteins that contain a signal peptide and any number of mono-basic or dibasic sites. The list obtained with NeuroPID was then used as a separate database for our mass spectrometry analysis to confirm hits without repetitive motifs. A list of proneuropeptides is provided in Supplementary file 2.

Peptidomics and mass spectrometry analysis

N. vectensis specimens were obtained from a culture maintained at the Marine Invertebrate Culture Unit at the University of Exeter. We processed four samples for peptidomics. Two samples contained larvae of different ages and primary polyps up to the age of 10 days. The other two samples contained juveniles and adult tissue. Feeding-stage animals were starved for two days prior to collection. All samples were quickly rinsed with Milli-Q water and snap-frozen in liquid nitrogen. Each sample was manually homogenized with a mortar and pestle in 10 ml of ice cold acidified methanol (90% methanol, 9% water, 1% acetic acid). The homogenate was collected and sonicated on dry ice for 4 x 15 sec with a 30 sec rest between cycles. Samples were centrifuged (10 minutes x 4000 g) and the supernatant transferred to a new tube. The

supernatant was concentrated in a vacuum concentrator until all methanol was evaporated. Samples were again centrifuged (10 minutes x 16,000 g) and the supernatant was twice delipidated, each time using 2 ml n-hexane and recovering the aqueous layer. Samples were then desalted with Pierce C18 spin columns following the manufacturer's guidelines and dried in a vacuum concentrator. Prior to LC-MS/MS analysis, samples were re-suspended in 5% acetonitrile, 95% water, 0.1% formic acid.

Samples were analyzed on a Waters nanoACQUITY UPLC coupled to a QExactive mass spectrometer (Thermo Scientific, Bremen, Germany) equipped with a nano-electrospray ion source. The column (µPAC™ trapping column, Thermo Scientific) was loaded with 5 µl of sample and set to a flow rate of 750 nl per minute. A linear gradient of solvent B (98% acetonitrile, 0.1% formic acid, 2% HPLC grade water) starting at 1% and increasing to 40% in solvent A (2% acetonitrile, 0.1% formic acid, 98% HPLC-grade water) over 80 minutes was used to separate peptides. MS data were acquired in a Top20 data-dependent acquisition mode with a dynamic exclusion of 20s. The most abundant precursor ions from a full scan MS were selected for higher-energy collisional dissociation (HCD) fragmentation.

Full MS1 scans were acquired with a resolution of 70,000 with automatic gain control (AGC) set to 3e+6, a maximum injection time of 100 ms and a scan range of 350-1850 m/z. The MS/MS fragmentation scans had a resolution of 17500, AGC of 1e+5, a maximum injection time of 80 ms and a normalized collision energy of 28.

Raw LC-MS/MS data were analyzed using PEAKS Studio X+ (v10.5 Bioinformatics Solutions Inc., Canada). Peptides were identified using a database of sequences generated from the entire secretome, the NeuroPID predictions and the predicted precursors from BLAST and motif searches. The precursor mass error tolerance was set to 5 ppm and the fragment mass error tolerance to 0.02 Da. The following variable post-translational modifications were included in the database search: pyroglutamation of N-terminal glutamic acid (-18.01 Da) or glutamine (-17.03 Da), C-terminal amidation (-0.98 Da) and half of a disulfide bridge on cysteine (-1.01 Da). Oxidation of methionine (+15.99 Da) was also included as a variable modification. Since the samples are not enzymatically digested, the database search parameters included “No Enzyme” and digest mode of “Unspecific”.

A false discovery rate of < 1% was applied to MS/MS peptide identifications and the resulting list of peptides was exported. Selection of candidate neuropeptides were based on the presence of a signal sequence in the precursor and of peptides being flanked or containing different potential cleavage site motifs. N-terminal cleavage site motifs included: KR/RR/RK/KK/EE/DD/ED/DE directly flanking the N-terminus of the peptide or Q, xP or xxP as the most N-terminal amino acid of the peptide (with x standing for a variable amino acid). C-terminal cleavage site motifs included KK/KR/RR/RK flanking the C-terminus of the peptide or GR/GK flanking the C-terminus of amidated peptides, with G denoting the donor of the amide group. The resulting list contained neuropeptide candidates where the MS/MS spectra were manually inspected to verify quality and confidence. To prioritize peptides for further investigation each identification was categorized as “confident”, “uncertain” or “poor”. "Confident" identifications were characterized by MS/MS spectra where peaks could be clearly distinguished from noise, the b and y ion ladders resolved amino acid masses with excellent peptide coverage missing at most one or two ions. "Uncertain" peptide identifications were characterized by having either (1) ion ladders with gaps of three amino acids but maintaining good overall coverage when the entire peptide

was considered or (2) the identified sequence overlapped with the predicted signal peptide or (3) disulfide bridges were present resulting in unresolved fragmentation between the cysteine-cysteine bond or (4) fragmentation was consistent with a confident peptide however the sequence was thought to be intermediate peptide requiring further biological processing. If MS/MS spectra had ion ladders with gaps larger than 3 amino acids or low intensity peaks the identification was considered "poor".
All mass spectrometric data are available through the PRIDE repository (Perez-Riverol et al., 2022) with accession number PXD041235. Peptides and details about detection, flanking amino acids, precursors sequences, categorized into "confident", "uncertain" and "poor" are provided in Supplementary file 1. Mass spectrometry pipeline infographic was created with BioRender.com (Supplementary figure 1A), MS/MS spectra and precursor annotation (Supplementary figure 1BC) figures exported from PEAKS Studio X+ (v10.5 Bioinformatics Solutions Inc., Canada).

GPCR sequence analysis

To identify potential neuropeptide receptors from the GPCR family A (the most extensive neuropeptide family), the full sequence alignment of the class A GPCRs (PF00001) was obtained from the PFAM database (https://pfam.xfam.org). The alignment was used to produce a Hidden Markov Model (HMM) with hmmer-3.1b2 (Eddy, 2011), which was then used to mine the proteomes from the species described above with an e-value cutoff of 1e−10. Redundant sequences were removed using CD-Hit (Eddy, 2011; Fu et al., 2012) with a similarity setting of 0.95. All GPCR protein sequences are provided in Supplementary file 6. The obtained sequences were analyzed using Phobius (Käll et al., 2007) to predict the number of transmembrane domains and only sequences with a minimum of four and maximum of nine transmembrane (TM) domains were kept for further analyses. The relationship between the obtained proteins from the different species was analyzed using an all-vs-all BLAST-based cluster strategy with the CLANS software (Eddy, 2011; Frickey and Lupas, 2004; Fu et al., 2012). The initial all-vs-all BLAST file was created using the online clans toolkit (https://toolkit.tuebingen.mpg.de/tools/clans), with the default BLOSUM62 scoring matrix and BLAST HSP's extracted up to E-values of 1e-14. The sequences were then clustered using the CLANS desktop version with a P-value cutoff of 1e-25 and color-coded according to taxonomy. Experimentally confirmed annotated sequences from human, *Drosophila melanogaster*, *Caenorhabditis elegans* and *Platynereis dumerilii* were used as reference sequences to annotate the cluster maps. Original cluster-map files including all sequences are provided in Figure 2–source data 1 and Figure 2–figure supplement 1–source data 1. *N. vectensis* sequences with connection to the bilaterian neuropeptide GPCR cluster or belonging to orphan clusters ancestral to cnidarians were cloned for experimental testing.
For the phylogenetic analysis, we extracted the sequences of the bilaterian and cnidarian neuropeptide GPCR cluster and those connected to it. As an outgroup, we chose a sub-cluster of monoamine receptors that showed the strongest connection to the main neuropeptide GPCR cluster. Initial analyses were done by aligning sequences with muscle (Edgar, 2004), trimming the alignment with the gappy-out function of TrimAl (Capella-Gutiérrez et al., 2009) and calculating trees with FastTree (Price et al., 2009) using the lg model. In subsequent analyses, we aligned the extracted genes with MAFFT v7 using the iterative refinement method E-INS-i

(Katoh et al., 2002). Alignments were trimmed with TrimAl in gappy-out mode and maximum likelihood trees calculated with IQ-tree2 with the LG + G4 model (Minh et al., 2020). Branch support was calculated by running 1,000 replicates with the aLRT-SH-like and aBayes methods. Protein sequences, untrimmed and trimmed alignments and tree files are provided in Figure 4–source data 1-4, Figure 4–figure supplement 1–source data 1-4, Figure 4–figure supplement 2–source data 1-4. The detailed trees shown in Figure 4 and Figure 4–figure supplement 1-2 with annotated branches are provided in Supplementary file 11.

GPCR and reporter gene cloning

All GPCRs were cloned from cDNA into the pcDNA3.1(+) vector either by standard cloning strategies based on restriction enzymes or by using the NEBuilder HiFi DNA Assembly kit. Genes that proved more problematic to clone were codon optimized and synthesized into a pcDNA3.1(+) vector by Genscript synthesis services. All tested GPCR sequences with individual cloning strategy, primers used and codon optimized sequences are provided in Supplementary file 8. The chimeric Gqi9 protein was ordered from Addgene (Plasmid No. 125711). This was then further modified using PCR and cloned into the pcDNA3.1(+) vector using the NEBuilder HiFi DNA Assembly kit. The reverse primer was engineered to change the most C-terminal amino acid residues Tyr-Cys-Gly-Leu-Cys to Asp-Cys-Gly-Leu-Phe, making it similar to the promiscuous chimeric Gqi5 protein (Conklin et al., 1993) yielding the vector pcDNA3.1-Gqi5/9. The chimeric G5A GFP-Aequorin protein (Baubet et al., 2000) was codon optimized for human cells and synthesized into a pcDNA 3.1(+) vector by Genscript. Codon-optimized G5A and Gqi5/9 sequences as well as cloning primers and further details are provided in Supplementary file 7.

Cell transfection and deorphanization assay

A detailed step-by-step protocol has been published in (Thiel et al., 2023). In brief, for transfection we used HEK293 cells that stably express the chimeric GFP-Aequorin protein G5A (CAT no. cAP-0200GFP-AEQ-Cyto). Cells were grown in 5% CO_2 atmosphere in DMEM (containing 4.5 g/l glucose, L-Glutamine, sodium pyruvate, Thermo; Cat. No. 10566016) supplemented with 10 % FBS (heat inactivated, Thermo; Cat. No. 10082147). A confluent T75 Flask of cells was transferred into 3-4 clear-bottom 96-well plates and grown for 2 days. At about 90% confluency, cells were transfected either with Transfectamine 5000 (T5000) or 25 kDA branched PEI (1 mg/ml), according to the protocol from Durocher 2002 (Durocher et al., 2002). The cell medium in the 96-well plates was exchanged with 90 µl of OptiMEM (supplemented with 5% FBS) prior to transfection. For each well, 10 µl OptiMEM (without FBS), 70 ng of GPCR containing plasmid, 70 ng of Gqi5/9 plasmid, 10-20 ng of G5A plasmid (to increase luminescence values of our HEK293 cell line), and 0.45-0.48 µl T5000/PEI were mixed and incubated for 20 min at room temperature. Transfection mixture was then added to the cells. Two days post transfection, the medium was removed and substituted with OptiMEM media supplemented with 4 µM coelenterazine-H (Promega; Cat. No. S2001), and incubated for

a period of 2 to 3 hours. Readings were performed with a FlexStation 3 Multi-mode Microplate reader (molecular devices), for a period of 60 sec per well, ligand injection after 15-18 sec, and the whole plate was read with the Flex option. We first tested different peptide mixes on each individual GPCR with a concentration of 10 µM per peptide. Receptors that were activated by any of these mixes were then tested with the individual peptides of the activating mix at a concentration of 10 µM. Individual peptides that activated a GPCR were then tested at different concentrations between 1e-13 M and 1e-4 M to obtain dose-response curves. Each peptide-receptor pair was tested in three independent triplicates. Supplementary file 3 contains the peptide mixes and Supplementary file 4 the test results of the peptide-mix screening assays. The readout data for the final dose-response curves is provided in Supplementary file 9 and as .csv files in the repository in the data folder. The data were analyzed in R with the drc package for curve fitting and EC_{50} calculations (Ritz et al., 2015). The scripts and the data in .csv format are provided on Zenodo (Thiel et al., 2024). The cells were tested for mycoplasma contamination by PCR.

Single Cell analysis

Gene models corresponding to all receptor-peptide pairs are not available in the version 1 genome and accompanying gene model set (https://figshare.com/articles/dataset/Nematostella_vectensis_transcriptome_and_gene_models_v2_0/807696), however all relevant gene models were identified within the Nv2 set of gene models that accompany the vs.2 chromosome level genome build (https://doi.org/10.1101/2020.10.30.359448). A single cell atlas dataset for *Nematostella*, mapped to this genome and Nv2 gene model set with corresponding clustering annotations is available (http://cells.ucsc.edu/?ds=sea-anemone-atlas; under an Nv2 subdirectory). Expression data for this gene set was extracted from this dataset, together with the cell clustering information. Expression profiles were visualized using the Seurat::DotPlot function for the both coarse tissue-level clustering, as well as cell-type clustering of the neuroglandular complement.

Network analysis

The multilayered peptidergic connectome was reconstructed based on the scRNAseq data from the developmental and adult subsets. We constructed an interaction network based on cell-specific average expression values of proneuropeptides and their receptors. Each cell type was a separate node in the network and connections were defined between a peptide-expressing and receptor-expressing cell based on the geometric mean of peptide and receptor expression, weighted by the absolute value of $\log_{10}EC_{50}$. We used the formula:

$$\sqrt{PeptideExpr \times ReceptorExpr} \times \left|log(EC_{50})\right|$$

Modules were identified with the Leiden algorithm (Traag et al., 2019). The network was visualized with the visNetwork package. The analysis was done with the script Figure6_and_Figure6_fig_suppl1.R.

Data and code availability

The scripts and data used for the dose-response curves, single cell analysis, clans analysis, phylogenetic trees, pattern searches and network analysis are available at (Thiel et al., 2024).

Supplementary and Supporting Material

The mass spectrometry proteomics data have been deposited to the ProteomeXchange Consortium via the PRIDE (Perez-Riverol et al., 2022) partner repository with the dataset identifier PXD041235 and 10.6019/PXD041235" .

Supplementary file 1: Mass spectrometry identification of *N. vectensis* neuropeptides. The table contains the results of the mass spectrometry analysis including the name, sequence and identifier of the precursor sequences, N- and C-terminal flanking sequences, and peptide sequences.

Supplementary file 2: *N. vectensis* proneuropeptides. The file contains a list of all *N. vectensis* proneuropeptide sequences identified in this study. Each precursor is provided with a list of alternative headers from the different resources, other studies that identified the same precursor, a list of peptides that were tested in this study, the receptors that were activated and cleavage site and signal peptides are indicated by different colors.

Supplementary file 3: Peptide mixes used for GPCR screening. The file contains the peptide mixes that were used in the initial peptide mix-GPCR screening (with additional information about the peptides and dilution of stock solutions).

Supplementary file 4: GPCR screening with peptide mixes. The file contains the data from the peptide mix-GPCR screening with the mixes (normalized as well as the original readings) and the readings to resolve those peptide mix-GPCR pairs that showed a positive signal and lead to the identification of the individual peptide-receptor pairs described in this study.

Supplementary file 5: Transcriptome resources. The file contains a list of the transcriptomes used in this study, together with the sources and data from the BUSCo analysis including completeness of the transcriptomes with percentage of single, double, fragmented and missing genes.

Supplementary file 6: Class A GPCR sequences. The file contains all GPCR sequences that were identified from the different taxa in the HMMer screening. In .fasta format.

Supplementary file 7: Gqi5/9 and G5A sequence. The file contains the nucleotide sequences of the Gqi5/9 and G5A gene with primer sequences and information about the mutation of the original Gqi9 that we obtained and subcloned into the pcDNA3.1(+) vector.

Supplementary file 8: Tested *N. vectensis* GPCR sequences. The file contains a list of all tested *N. vectensis* GPCRs, including original nucleotide and protein sequences, information about the cloning strategy and either the primer sequences of genes that we cloned ourselves or the codon-optimized sequences of genes that were ordered as synthetic constructs.

Supplementary file 9: Dose-response assay readings. The file contains the original readings from our dose-response curves as well as additional measurements such as those for supplementary figures or of peptide-receptor pairs that initially gave a signal in our screen but did not produce confident dose-response curves, as well as negative controls from peptides that were tested at different concentrations on cells that were only transfected with G5A and Gqi5/9 containing plasmids.

Supplementary file 10: EC_{50} values and curve slopes. The file contains the EC_{50} values and slopes of the dose-response curves for each peptide-receptor pair.

Supplementary file 11: Trees of sequences related to class A neuropeptide GPCRs. The file contains the detailed trees that are shown in Figure 4 and Figure 4–figure supplement 1 and 2, with exact support values and sequence identifiers of all branches.

Supplementary file 12: Single-cell analysis of *N. vectensis* neuropeptide precursors and GPCRs. The file contains the detailed dotplots of Figure 5 with cell-type resolution of the developmental and the adult single cell dataset.

References

Alzugaray ME, Adami ML, Diambra LA, Hernandez-Martinez S, Damborenea C, Noriega FG, Ronderos JR. 2013. Allatotropin: an ancestral myotropic neuropeptide involved in feeding. *PLoS One* **8**:e77520.

Alzugaray ME, Bruno MC, Villalobos Sambucaro MJ, Ronderos JR. 2019. The Evolutionary History of The Orexin/Allatotropin GPCR Family: from Placozoa and Cnidaria to Vertebrata. *Sci Rep* **9**:10217.

Anctil M. 2009. Chemical transmission in the sea anemone Nematostella vectensis: A genomic perspective. *Comp Biochem Physiol Part D Genomics Proteomics* **4**:268–289.

Artigas GQ, Lapébie P, Leclère L, Bauknecht P, Uveira J, Chevalier S, Jékely G, Momose T, Houliston E. 2020. A G protein–coupled receptor mediates neuropeptide-induced oocyte maturation in the jellyfish Clytia. *PLOS Biology*. doi:10.1371/journal.pbio.3000614

Assmann M, Kuhn A, Dürrnagel S, Holstein TW, Gründer S. 2014. The comprehensive analysis of DEG/ENaC subunits in Hydra reveals a large variety of peptide-gated channels, potentially involved in neuromuscular transmission. *BMC Biol* **12**:84.

Baubet V, Le Mouellic H, Campbell AK, Lucas-Meunier E, Fossier P, Brúlet P. 2000. Chimeric

green fluorescent protein-aequorin as bioluminescent Ca2+ reporters at the single-cell level. *Proc Natl Acad Sci U S A* **97**:7260–7265.
Bauknecht P, Jékely G. 2017. Ancient coexistence of norepinephrine, tyramine, and octopamine signaling in bilaterians. *BMC Biol* **15**:6.
Beets I, Zels S, Vandewyer E, Demeulemeester J, Caers J, Baytemur E, Schafer WR, Vértes PE, Mirabeau O, Schoofs L. 2022. System-wide mapping of neuropeptide-GPCR interactions in*C. elegans*. doi:10.1101/2022.10.30.514428
Bentley B, Branicky R, Barnes CL, Chew YL, Yemini E, Bullmore ET, Vértes PE, Schafer WR. 2016. The Multilayer Connectome of Caenorhabditis elegans. *PLoS Comput Biol* **12**:e1005283.
Bosch TCG, Klimovich A, Domazet-Lošo T, Gründer S, Holstein TW, Jékely G, Miller DJ, Murillo-Rincon AP, Rentzsch F, Richards GS, Schröder K, Technau U, Yuste R. 2017. Back to the Basics: Cnidarians Start to Fire. *Trends Neurosci* **40**:92–105.
Capella-Gutiérrez S, Silla-Martínez JM, Gabaldón T. 2009. trimAl: a tool for automated alignment trimming in large-scale phylogenetic analyses. *Bioinformatics* **25**:1972–1973.
Chufán EE, De M, Eipper BA, Mains RE, Amzel LM. 2009. Amidation of bioactive peptides: the structure of the lyase domain of the amidating enzyme. *Structure* **17**:965–973.
Cole AG, Jahnel SM, Kaul S, Steger J, Hagauer J, Denner A, Murguia PF, Taudes E, Zimmermann B, Reischl R, Steinmetz PRH, Technau U. 2023. Muscle cell-type diversification is driven by bHLH transcription factor expansion and extensive effector gene duplications. *Nat Commun* **14**:1747.
Cole AG, Steger J, Hagauer J, Denner A, Murguia PF, Knabl P, Narayanaswamy S, Wick B, Montenegro JD, Technau U. 2024. Updated single cell reference atlas for the starlet anemone Nematostella vectensis. doi:10.21203/rs.3.rs-3854371/v1
Conklin BR, Farfel Z, Lustig KD, Julius D, Bourne HR. 1993. Substitution of three amino acids switches receptor specificity of Gq alpha to that of Gi alpha. *Nature* **363**:274–276.
Dandamudi M, Hausen H, Lynagh T. 2022. Comparative analysis defines a broader FMRFamide-gated sodium channel family and determinants of neuropeptide sensitivity. *J Biol Chem* **298**:102086.
Deng B, Li Q, Liu X, Cao Y, Li B, Qian Y, Xu R, Mao R, Zhou E, Zhang W, Huang J, Rao Y. 2019. Chemoconnectomics: Mapping Chemical Transmission in Drosophila. *Neuron* **101**:876–893.e4.
Dennerlein S, Oeljeklaus S, Jans D, Hellwig C, Bareth B, Jakobs S, Deckers M, Warscheid B, Rehling P. 2015. MITRAC7 Acts as a COX1-Specific Chaperone and Reveals a Checkpoint during Cytochrome c Oxidase Assembly. *Cell Rep* **12**:1644–1655.
de Oliveira AL, Calcino A, Wanninger A. 2019. Ancient origins of arthropod moulting pathway components. *Elife* **8**. doi:10.7554/eLife.46113
Durocher Y, Perret S, Kamen A. 2002. High-level and high-throughput recombinant protein production by transient transfection of suspension-growing human 293-EBNA1 cells. *Nucleic Acids Res* **30**:E9.
Eddy SR. 2011. Accelerated Profile HMM Searches. *PLoS Comput Biol* **7**:e1002195.
Edgar RC. 2004. MUSCLE: a multiple sequence alignment method with reduced time and space complexity. *BMC Bioinformatics* **5**:113.
Elkhatib W, Yanez-Guerra LA, Mayorova TD, Currie MA, Perera M, Singh A, Gauberg J, Senatore A. 2022. Function and phylogeny support the independent evolution of acid-sensing ion channels in the Placozoa. *bioRxiv*. doi:10.1101/2022.06.28.497943
Elphick MR, Mirabeau O. 2014. The Evolution and Variety of RFamide-Type Neuropeptides: Insights from Deuterostomian Invertebrates. *Front Endocrinol* **5**:93.
Elphick MR, Mirabeau O, Larhammar D. 2018. Evolution of neuropeptide signalling systems. *J Exp Biol* **221**. doi:10.1242/jeb.151092
Escudero Castelán N, Semmens DC, Guerra LAY, Zandawala M, Dos Reis M, Slade SE,

Scrivens JH, Zampronio CG, Jones AM, Mirabeau O, Elphick MR. 2022. Receptor deorphanization in an echinoderm reveals kisspeptin evolution and relationship with SALMFamide neuropeptides. *BMC Biol* **20**:187.
Fredriksson R, Schiöth HB. 2005. The Repertoire of G-Protein–Coupled Receptors in Fully Sequenced Genomes. *Molecular Pharmacology*. doi:10.1124/mol.104.009001
Frickey T, Lupas A. 2004. CLANS: a Java application for visualizing protein families based on pairwise similarity. *Bioinformatics* **20**:3702–3704.
Fu L, Niu B, Zhu Z, Wu S, Li W. 2012. CD-HIT: accelerated for clustering the next-generation sequencing data. *Bioinformatics* **28**:3150–3152.
Gilbert E, Teeling C, Lebedeva T, Pedersen S, Chrismas N, Genikhovich G, Modepalli V. 2022. Molecular and cellular architecture of the larval sensory organ in the cnidarian Nematostella vectensis. *Development* **149**. doi:10.1242/dev.200833
Grimmelikhuijzen CJP, Hauser F. 2012. Mini-review: the evolution of neuropeptide signaling. *Regul Pept* **177 Suppl**:S6–9.
Grimmelikhuijzen CJ, Rinehart KL, Jacob E, Graff D, Reinscheid RK, Nothacker HP, Staley AL. 1990. Isolation of L-3-phenyllactyl-Leu-Arg-Asn-NH2 (Antho-RNamide), a sea anemone neuropeptide containing an unusual amino-terminal blocking group. *Proc Natl Acad Sci U S A* **87**:5410–5414.
Gründer S, Ramírez AO, Jékely G. 2022. Neuropeptides and DEG/ENaC ion channels: a relationship from mammals to cnidarians. *J Physiol*. doi:10.1113/jp282309
Hauser F, Koch TL, Grimmelikhuijzen CJP. 2022. Review: The evolution of peptidergic signaling in Cnidaria and Placozoa, including a comparison with Bilateria. *Front Endocrinol* **13**:973862.
Hayakawa E, Guzman C, Horiguchi O, Kawano C, Shiraishi A, Mohri K, Lin M-F, Nakamura R, Nakamura R, Kawai E, Komoto S, Jokura K, Shiba K, Shigenobu S, Satake H, Inaba K, Watanabe H. 2022. Mass spectrometry of short peptides reveals common features of metazoan peptidergic neurons. *Nat Ecol Evol*. doi:10.1038/s41559-022-01835-7
Hayakawa E, Watanabe H, Menschaert G, Holstein TW, Baggerman G, Schoofs L. 2019. A combined strategy of neuropeptide prediction and tandem mass spectrometry identifies evolutionarily conserved ancient neuropeptides in the sea anemone Nematostella vectensis. *PLoS One* **14**:e0215185.
Ikmi A, McKinney SA, Delventhal KM, Gibson MC. 2014. TALEN and CRISPR/Cas9-mediated genome editing in the early-branching metazoan Nematostella vectensis. *Nat Commun* **5**:5486.
Jékely G. 2021. The chemical brain hypothesis for the origin of nervous systems. *Philos Trans R Soc Lond B Biol Sci* **376**:20190761.
Jékely G. 2013. Global view of the evolution and diversity of metazoan neuropeptide signaling. *Proc Natl Acad Sci U S A* **110**:8702–8707.
Käll L, Krogh A, Sonnhammer ELL. 2007. Advantages of combined transmembrane topology and signal peptide prediction--the Phobius web server. *Nucleic Acids Res* **35**:W429–32.
Katoh K, Misawa K, Kuma K-I, Miyata T. 2002. MAFFT: a novel method for rapid multiple sequence alignment based on fast Fourier transform. *Nucleic Acids Res* **30**:3059–3066.
Koch TL, Grimmelikhuijzen CJP. 2020. A comparative genomics study of neuropeptide genes in the cnidarian subclasses Hexacorallia and Ceriantharia. *BMC Genomics* **21**:666.
Koch TL, Grimmelikhuijzen CJP. 2019. Global Neuropeptide Annotations From the Genomes and Transcriptomes of Cubozoa, Scyphozoa, Staurozoa (Cnidaria: Medusozoa), and Octocorallia (Cnidaria: Anthozoa). *Front Endocrinol* **10**:831.
Koch TL, Hauser F, Grimmelikhuijzen CJP. 2021. An evolutionary genomics view on neuropeptide genes in Hydrozoa and Endocnidozoa (Myxozoa). *BMC Genomics* **22**:862.
Krishnan A, Schiöth HB. 2015. The role of G protein-coupled receptors in the early evolution of neurotransmission and the nervous system. *J Exp Biol* **218**:562–571.

Li W, Godzik A. 2006. Cd-hit: a fast program for clustering and comparing large sets of protein or nucleotide sequences. *Bioinformatics* **22**:1658–1659.
Minh BQ, Schmidt HA, Chernomor O, Schrempf D, Woodhams MD, von Haeseler A, Lanfear R. 2020. IQ-TREE 2: New Models and Efficient Methods for Phylogenetic Inference in the Genomic Era. *Mol Biol Evol* **37**:1530–1534.
Mirabeau O, Joly J-S. 2013. Molecular evolution of peptidergic signaling systems in bilaterians. *Proc Natl Acad Sci U S A* **110**:E2028–37.
Moroz LL, Romanova DY, Kohn AB. 2021. Neural versus alternative integrative systems: molecular insights into origins of neurotransmitters. *Philos Trans R Soc Lond B Biol Sci* **376**:20190762.
Nakanishi N, Martindale MQ. 2018. CRISPR knockouts reveal an endogenous role for ancient neuropeptides in regulating developmental timing in a sea anemone. *Elife* **7**. doi:10.7554/eLife.39742
Nikitin M. 2015. Bioinformatic prediction of Trichoplax adhaerens regulatory peptides. *Gen Comp Endocrinol* **212**:145–155.
Ofer D, Linial M. 2014. NeuroPID: a predictor for identifying neuropeptide precursors from metazoan proteomes. *Bioinformatics* **30**:931–940.
Paix A, Basu S, Steenbergen P, Singh R, Prevedel R, Ikmi A. 2023. Endogenous tagging of multiple cellular components in the sea anemone. *Proc Natl Acad Sci U S A* **120**:e2215958120.
Perez-Riverol Y, Bai J, Bandla C, García-Seisdedos D, Hewapathirana S, Kamatchinathan S, Kundu DJ, Prakash A, Frericks-Zipper A, Eisenacher M, Walzer M, Wang S, Brazma A, Vizcaíno JA. 2022. The PRIDE database resources in 2022: a hub for mass spectrometry-based proteomics evidences. *Nucleic Acids Res* **50**:D543–D552.
Price MN, Dehal PS, Arkin AP. 2009. FastTree: computing large minimum evolution trees with profiles instead of a distance matrix. *Mol Biol Evol* **26**:1641–1650.
Regard JB, Sato IT, Coughlin SR. 2008. Anatomical Profiling of G Protein-Coupled Receptor Expression. *Cell*. doi:10.1016/j.cell.2008.08.040
Ritz C, Baty F, Streibig JC, Gerhard D. 2015. Dose-Response Analysis Using R. *PLoS One* **10**:e0146021.
Roch GJ, Sherwood NM. 2014. Glycoprotein Hormones and Their Receptors Emerged at the Origin of Metazoans. *Genome Biology and Evolution*. doi:10.1093/gbe/evu118
Sachkova MY, Nordmann E-L, Soto-Àngel JJ, Meeda Y, Górski B, Naumann B, Dondorp D, Chatzigeorgiou M, Kittelmann M, Burkhardt P. 2021. Neuropeptide repertoire and 3D anatomy of the ctenophore nervous system. *Curr Biol* **31**:5274–5285.e6.
Sanders SM, Ma Z, Hughes JM, Riscoe BM, Gibson GA, Watson AM, Flici H, Frank U, Schnitzler CE, Baxevanis AD, Nicotra ML. 2018. CRISPR/Cas9-mediated gene knockin in the hydroid Hydractinia symbiolongicarpus. *BMC Genomics* **19**:649.
Seidah NG. 2011. The proprotein convertases, 20 years later. *Methods Mol Biol* **768**:23–57.
Semmens DC, Beets I, Rowe ML, Blowes LM, Oliveri P, Elphick MR. 2015. Discovery of sea urchin NGFFFamide receptor unites a bilaterian neuropeptide family. *Open Biol* **5**:150030.
Smith SJ, Sümbül U, Graybuck LT, Collman F, Seshamani S, Gala R, Gliko O, Elabbady L, Miller JA, Bakken TE, Rossier J, Yao Z, Lein E, Zeng H, Tasic B, Hawrylycz M. 2019. Single-cell transcriptomic evidence for dense intracortical neuropeptide networks. *Elife* **8**. doi:10.7554/eLife.47889
Soave M, Stoddart LA, White CW, Kilpatrick LE, Goulding J, Briddon SJ, Hill SJ. 2021. Detection of genome-edited and endogenously expressed G protein-coupled receptors. *FEBS J* **288**:2585–2601.
Southey BR, Sweedler JV, Rodriguez-Zas SL. 2008. Prediction of neuropeptide cleavage sites in insects. *Bioinformatics* **24**:815–825.
Sriram K, Wiley SZ, Moyung K, Gorr MW, Salmerón C, Marucut J, French RP, Lowy AM, Insel

PA. 2019. Detection and Quantification of GPCR mRNA: An Assessment and Implications of Data from High-Content Methods. *ACS Omega* **4**:17048–17059.
Steger J, Cole AG, Denner A, Lebedeva T, Genikhovich G, Ries A, Reischl R, Taudes E, Lassnig M, Technau U. 2022. Single-cell transcriptomics identifies conserved regulators of neuroglandular lineages. *Cell Rep* **40**:111370.
Taylor SR, Santpere G, Weinreb A, Barrett A, Reilly MB, Xu C, Varol E, Oikonomou P, Glenwinkel L, McWhirter R, Poff A, Basavaraju M, Rafi I, Yemini E, Cook SJ, Abrams A, Vidal B, Cros C, Tavazoie S, Sestan N, Hammarlund M, Hobert O, Miller DM 3rd. 2021. Molecular topography of an entire nervous system. *Cell* **184**:4329–4347.e23.
Thiel D, Franz-Wachtel M, Aguilera F, Hejnol A. 2018. Xenacoelomorph Neuropeptidomes Reveal a Major Expansion of Neuropeptide Systems during Early Bilaterian Evolution. *Molecular Biology and Evolution*. doi:10.1093/molbev/msy160
Thiel D, Yañez-Guerra LA, Franz-Wachtel M, Hejnol A, Jékely G. 2021. Nemertean, Brachiopod, and Phoronid Neuropeptidomics Reveals Ancestral Spiralian Signaling Systems. *Mol Biol Evol* **38**:4847–4866.
Thiel D, Yañez-Guerra LA, Jékely G. 2024. Code documentation for “Large-scale deorphanization of Nematostella vectensis neuropeptide GPCRs supports the independent expansion of bilaterian and cnidarian peptidergic systems.” Zenodo. doi:10.5281/ZENODO.10680381
Thiel D, Yañez-Guerra LA, Jekely G. 2023. GPCR deorphanization assay in HEK-293 cells. *Bio Protoc*. doi:10.21769/p2493
Traag VA, Waltman L, van Eck NJ. 2019. From Louvain to Leiden: guaranteeing well-connected communities. *Sci Rep* **9**:5233.
Veenstra JA. 2000. Mono- and dibasic proteolytic cleavage sites in insect neuroendocrine peptide precursors. *Arch Insect Biochem Physiol* **43**:49–63.
Walker RJ, Papaioannou S, Holden-Dye L. 2009. A review of FMRFamide- and RFamide-like peptides in metazoa. *Invert Neurosci* **9**:111–153.
Williams EA. 2020. Function and Distribution of the Wamide Neuropeptide Superfamily in Metazoans. *Front Endocrinol* **11**:344.
Williams EA, Verasztó C, Jasek S, Conzelmann M, Shahidi R, Bauknecht P, Mirabeau O, Jékely G. 2017. Synaptic and peptidergic connectome of a neurosecretory center in the annelid brain. *Elife* **6**. doi:10.7554/eLife.26349
Wittlieb J, Khalturin K, Lohmann JU, Anton-Erxleben F, Bosch TCG. 2006. Transgenic Hydra allow in vivo tracking of individual stem cells during morphogenesis. *Proc Natl Acad Sci U S A* **103**:6208–6211.
Yañez-Guerra LA, Elphick MR. 2020. Evolution and Comparative Physiology of Luqin-Type Neuropeptide Signaling. *Front Neurosci* **14**:130.
Yañez-Guerra LA, Thiel D, Jékely G. 2022. Premetazoan Origin of Neuropeptide Signaling. *Mol Biol Evol* **39**. doi:10.1093/molbev/msac051

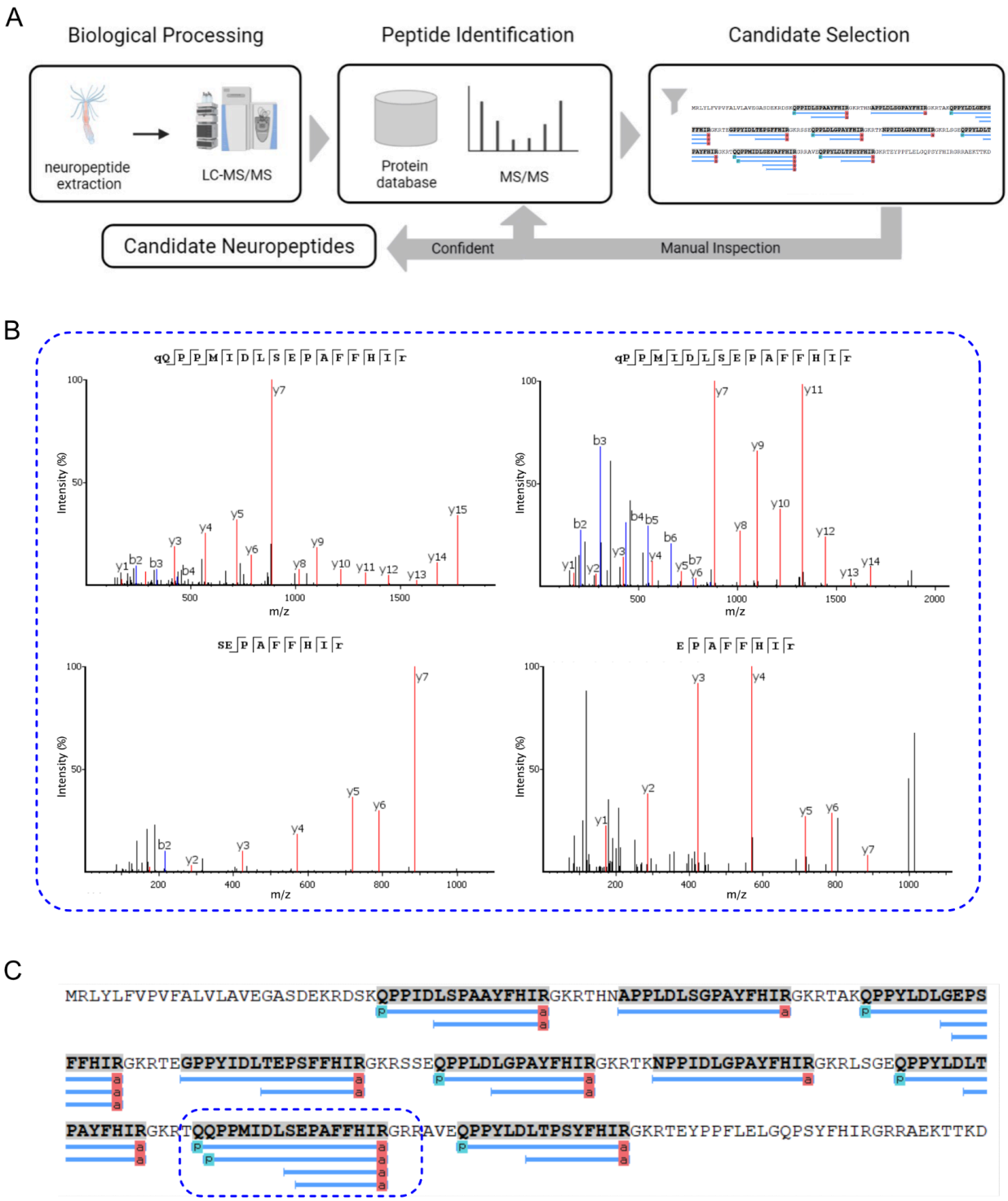

Figure 1–figure supplement 1: Mass spectrometry pipeline. (**A**) Pipeline for mass spectrometry identification of neuropeptide candidates. (**B**) Example spectra of detected HIRamide peptides with different lengths that originate from the same peptide on the HIRamide precursor. The shown spectra are from the encircled HIRamide peptide copy in (C). (**C**) HIRamide precursor with different HIRamide peptides indicated as a blue line below the precursor sequence.

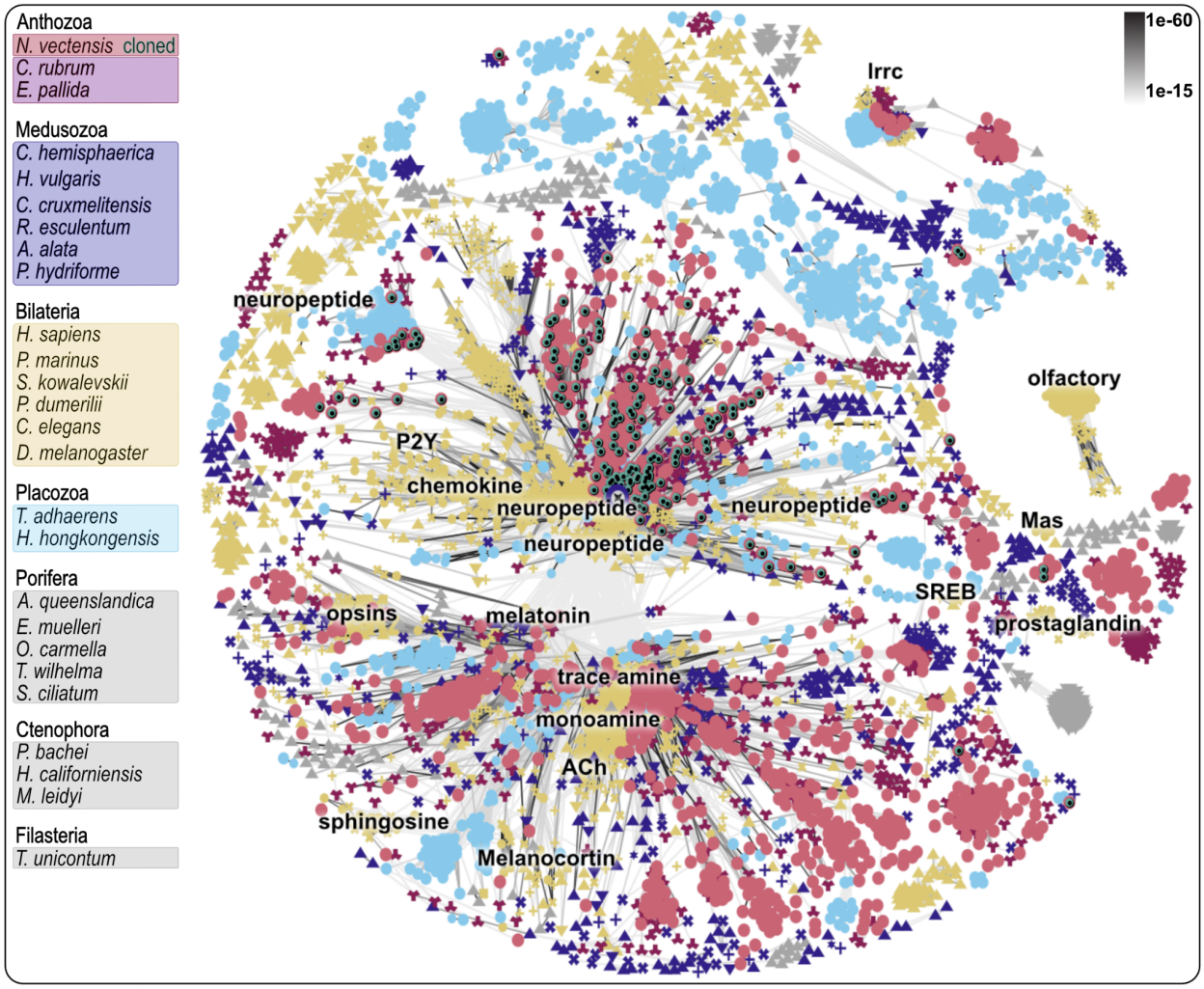

Figure 2–figure supplement 1: Clustermap of metazoan class A GPCRs. Each dot represents a GPCR sequence with color-coding according to Species list on the left. Connecting lines between single sequences show similarity with P-values indicated in top right. Annotations are based on sequences of deorphanized bilaterian class A GPCRs. Abbreviations in C: ACh = acetylcholine, lrrc = leucine rich repeat containing, P2Y = purinergic P2Y receptor.
Figure 2–figure supplement 1–source data 1. Raw cluster analysis CLANS file.

A

	GPR21 (original readings)	GPR21 (1e−13 set to zero)	GPR29
	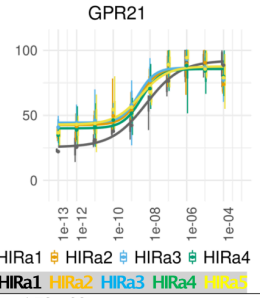	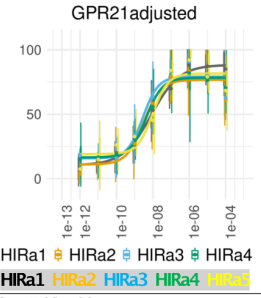	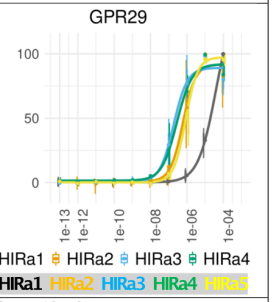
HIRa1 (pyro-QPPYLDLGEPSFFHIR-amide)	EC_{50}=1.59e-09	EC_{50}=5.93e-09	EC_{50}=4.12e-05
HIRa2 (YPPFLELGQPSYFHIR-amide)	EC_{50}=1.15e-11	EC_{50}=3.1e-09	EC_{50}=5.96e-07
HIRa3 (pyro-QPPYLDLTPAYFHIR-amide)	EC_{50}=7.64e-12	EC_{50}=2.07e-09	EC_{50}=1.86e-07
HIRa4 (pyro-QPPLDLGPAYFHIR-amide)	EC_{50}=3.37e-11	EC_{50}=3.43e-09	EC_{50}=2.78e-07
HIRa5 (NPPIDLGPAYFHIR-amide)	EC_{50}=1.08e-11	EC_{50}=2.96e-09	EC_{50}=8.48e-07

B

MRLYLFVPVFALVLAVEGASDEKRDSKQPPIDLSPAAYFHIRGKRTYNAPPLDLSGPAYFHIRGKRTAKQPPYLDLGEPSFFHIRGKRTEGPPYIDLTEPSFFHIRGKRSSEQPPLDLGPAYFHIRGK
RTKNPPIDLGPAYFHIRGKRLSGEQPPYLDLTPAYFHIRGKRTQQPPMIDLSEPAFFHIRGRRAVEQPPYLDLTPSYFHIRGKRTEYPPFLELGQPSYFHIRGRRAEKTTKD

Figure 3–figure supplement 1: Dose response curves with EC_{50} values and peptide precursor of different HIRamide peptides. (**A**) Dose response curves of HIRamide peptide and GPR 21 + 29. Dose response curves show activation of receptors GPR21 and GPR29 with different HIRamide peptide versions from the same precursor. Sequences and EC_{50} values for different HIRamides are shown below the dose response curves. The graph in Figure 3 shows HIRamide3 as the peptide with the lowest EC_{50} values. GPR21 showed already at low concentrations a high base activation compared to the negative control, but did not show a clear increase in intensity at concentrations between 1e-13 and 1e-11. We therefore set the minimum to the value measured at a concentration of 1e-13 instead of the negative control and show a comparison of the corresponding graphs and EC_{50} values here. (**B**) HIRamide precursor. The N-terminal signal peptide of the precursors sequence is not highlighted, cleavage + amidation sites are highlighted in a darker gray. Tested peptides are underlined and coloured as shown underneath the dose response curves.
Figure 3–figure supplement 1–source data 1. Tibble with all data points used to calculate the Dose-response curves and EC_{50} values, in .csv format.

A

	GPR28	GPR32
	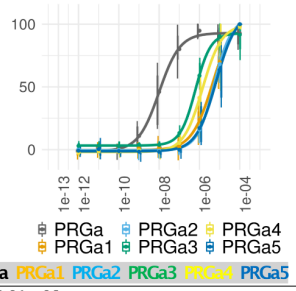	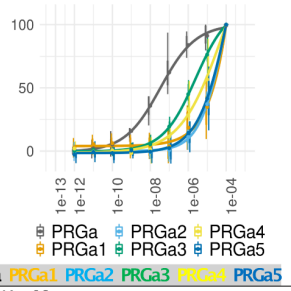
PRGa (GPRG–amide)	EC_{50}=1.01e–08	EC_{50}=3.41e–08
PRGa1 (APRGGRSLLDLLAAPRG–amide)	EC_{50}=4.69e–06	EC_{50}=7.99e–05
PRGa2 (GPRGGREVNLEGPRG–amide)	EC_{50}=5.34e–06	EC_{50}=9.51e–05
PRGa3 (GPRGGRATEFGPRG–amide)	EC_{50}=6.29e–07	EC_{50}=2.49e–06
PRGa4 (GPRGGRSYDGPRG–amide)	EC_{50}=1.43e–06	EC_{50}=2.15e–05
PRGa5 (APRGGRDAPRG–amide)	EC_{50}=6.69e–06	EC_{50}=1.34e–04

B

MAYFKWTLCAFVLAVLCLSTNYVAGEKNEEKSEKSTLLQELSKKDFDKELAADEAIVLELLKEKADDLDEESLLDLLAPRGGRDAPRGGRSLLDAPRGGRSLLDLLAAPRGGRDAPRGGRSLTELLNA
PRRGRSLADLLDAPRGGRSLAELLDAPRGGRSIEAPRGGRSLAELLEAPRGGRSLIELLEAPRGGRSVEAPRGGRSILELLTAPRGGRSAPRGGRSAEKSDAIHKEKKAPRGGRKRRSLPEEEMDGPR
GGRSAVSGRSSEDGPRGGRAVYGPRGGRSFDGSRGGRSYDGPRGGRSMENGPRGGRATEFGPRGGRSYEGSRGGREIDGPRGGRSFKEGPRGGRAVEGPRGGRDLYEEGPRGGREVYLEGPRGGRDLV
LEGPRGGRDLYEEGPRGGREVNLEGPRGGRDLYEEGPRGGRSYDGPRGGRSMENGRSAVYGPRGGRDANDGPRGGRDANDGPRGGRDANDGPRGGRDANEGPRGGRDANEGPRGGRDANKGPRGGRNTNTVGAQ
QADARQGQRGGRSTGMGPRGGRSVSSEKDNRH

Figure 3–figure supplement 2: Dose response curves with EC_{50} values and peptide precursor of different PRGamide peptide versions for two of the PRGamide receptors. (**A**) Dose response curves show activation of the receptors GPR28 and GPR32 with different PRGamide peptide versions from the same precursor. Sequences and EC_{50} values for different PRGamides are shown below the dose response curves. The graph in Figure 3 shows the shortest PRGamide (GPRG-amide) as the peptide with the lowest EC_{50} values, which is likely the fully processed version. (**B**) PRGamide precursor. The N-terminal signal peptide of the precursor sequence is not highlighted, cleavage and amidation sites are highlighted in a darker gray. The tested peptides are coloured to match the color of the dose response curves and the GPRG peptide is underlined.
Source data file is the same as for Figure 3–figure supplement 1.

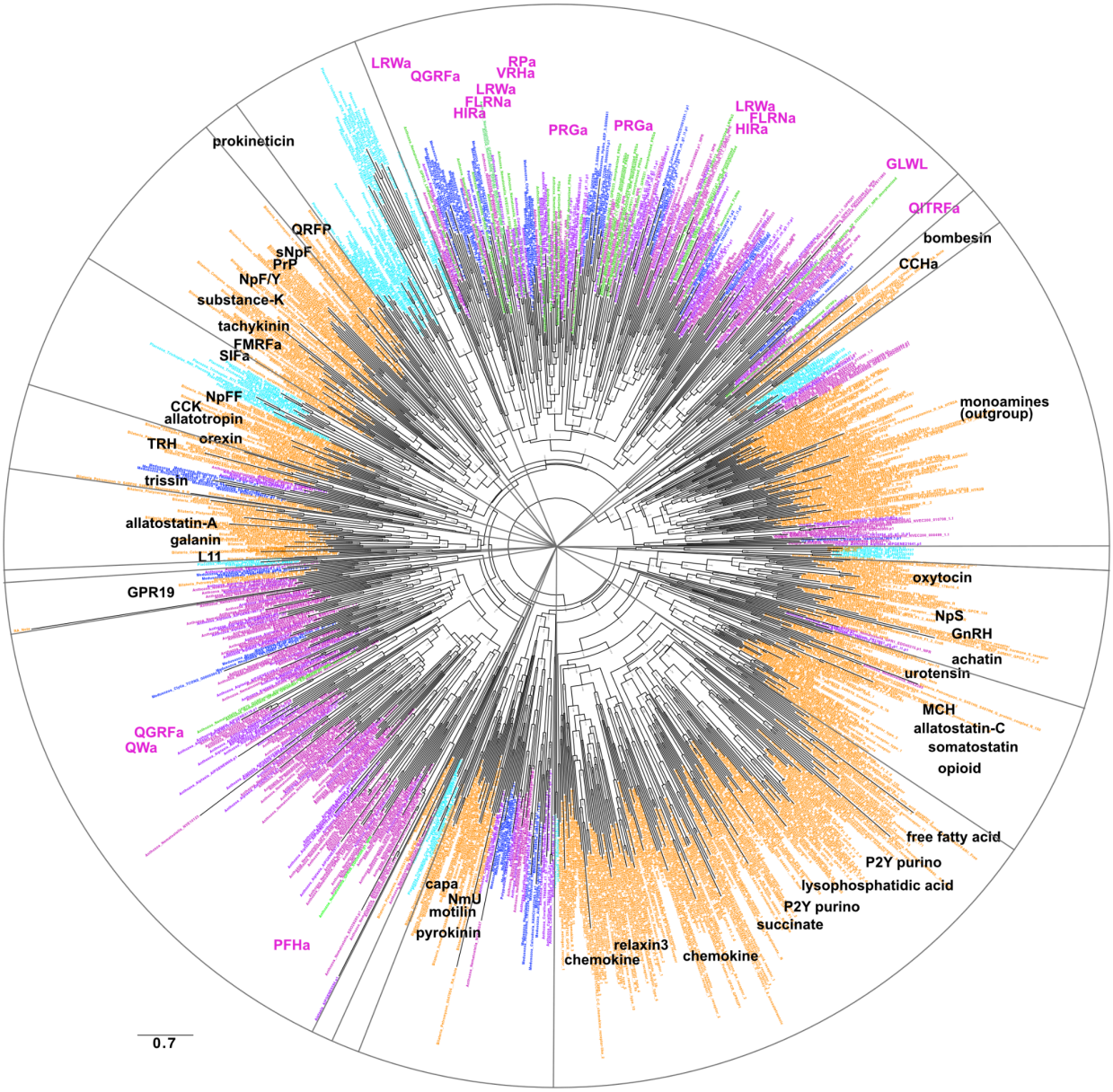

Figure 4–figure supplement 1: Tree (FastTree) of neuropeptide GPCRs with bilaterian chemokine and related receptors. Bilaterian sequences are shown in yellow, cnidarian sequences are shown in dark blue (Medusozoa) and magenta (Anthozoa), placozoan sequences are shown in light blue. Deorphanized *Nematostella vectensis* sequences are shown in green. Sequences were aligned using muscle, alignment was trimmed with the gappyout option of trimal, tree was calculated using FastTree. Abbreviations: a = amide, CCK = cholecystokinin, GnRH = gonadotropn releasing hormone, GPR19 = G protein-coupled receptor 19, L11 = elevenin, MCH = melanin concentrating hormone, Nm-U = neuromedin U, NpFF = neuropeptide FF, NpS = neuropeptide S, NpY/F = neuropeptide Y/neuropeptide F, PrP = prolactin releasing peptide, sNpF = short neuropeptide F, TRH = thyrotropin releasing hormone.
Figure 4–figure supplement 1–source data 1. Raw sequences used for tree building, .fasta format.
Figure 4–figure supplement 1–source data 2. Aligned sequences used for tree building.
Figure 4–figure supplement 1–source data 3. Trimmed sequence alignment used for tree

building.
Figure 4–figure supplement 1–source data 4. Tree file in nexus format.

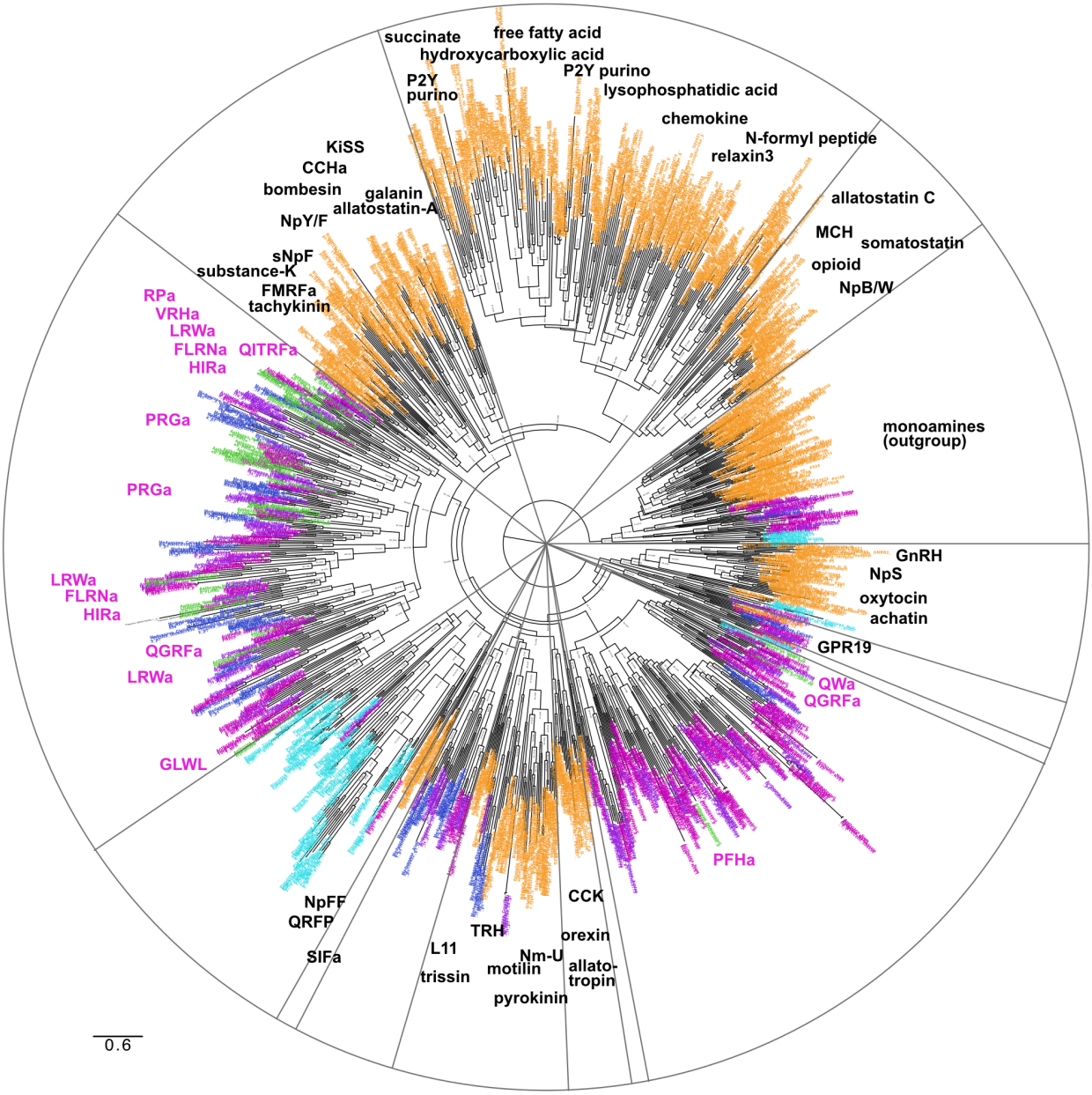

Figure 4–figure supplement 2: Tree (IQtree) of neuropeptide GPCRs with bilaterian chemokine and related receptors. Bilaterian sequences are shown in yellow, cnidarian sequences are shown in dark blue (Medusozoa) and magenta (Anthozoa), placozoan sequences are shown in light blue. Deorphanized *Nematostella vectensis* sequences are shown in green. Sequences were aligned using mafft, alignment was trimmed with the gappyout option of trimal, tree was calculated using IQtree. Abbreviations: a = amide, CCK = cholecystokinin,

GnRH = gonadotropin releasing hormone, GPR19 = G protein-coupled receptor 19, L11 = elevenin, MCH = melanin concentrating hormone, Nm-U = neuromedin U, NpB/W = neuropeptide B/neuropeptide W, NpFF = neuropeptide FF, NpS = neuropeptide S, NpY/F = neuropeptide Y/neuropeptide F, sNpF = short neuropeptide F.
Figure 4–figure supplement 2–source data 1. Raw sequences used for tree building, .fasta format.
Figure 4–figure supplement 2–source data 2. Aligned sequences used for tree building.
Figure 4–figure supplement 2–source data 3. Trimmed sequence alignment used for tree building.
Figure 4–figure supplement 2–source data 4. Tree file in nexus format.

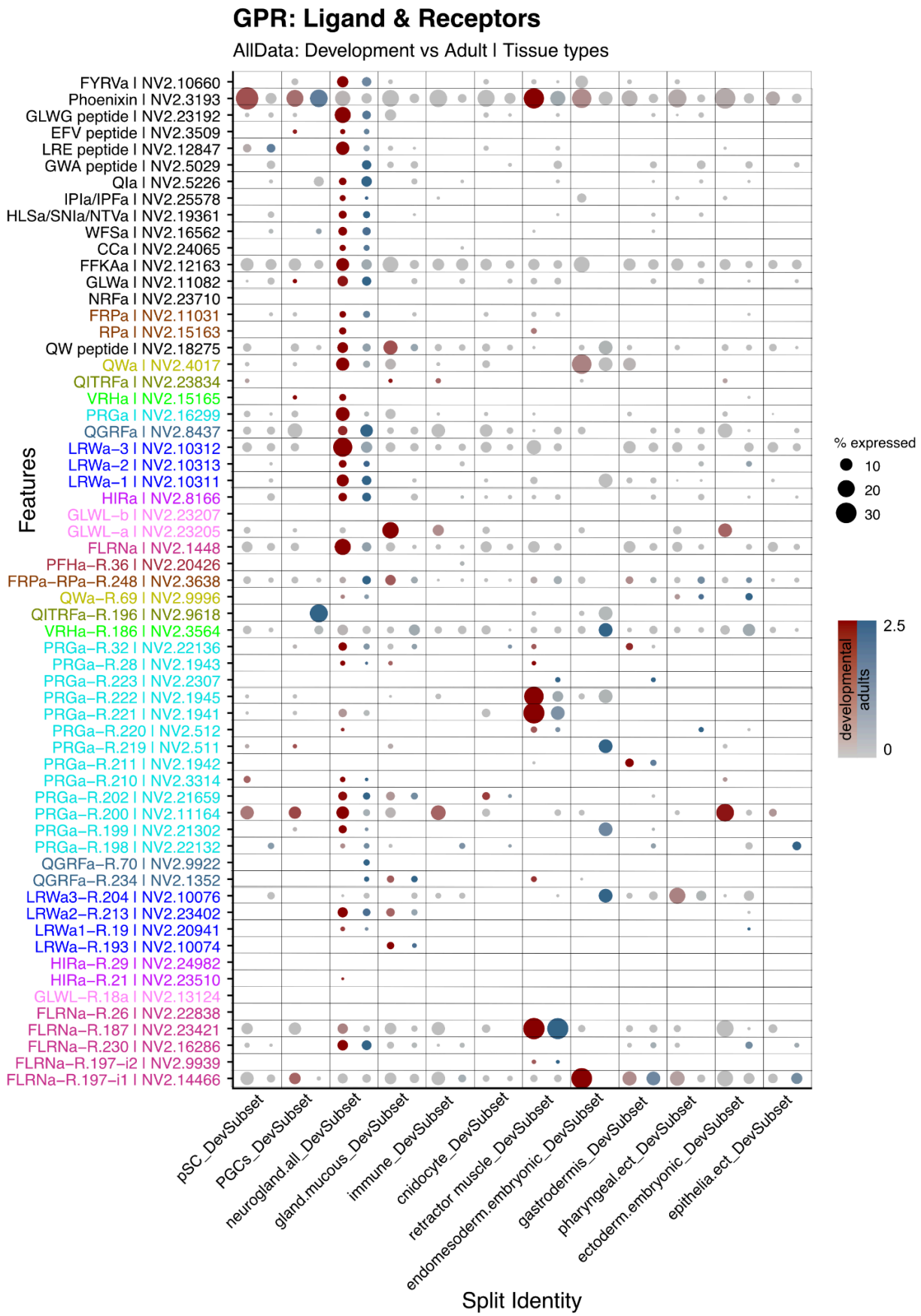
GPR: Ligand & Receptors
AllData: Development vs Adult | Tissue types
Features
FYRVa | NV2.10660
Phoenixin | NV2.3193
GLWG peptide | NV2.23192
EFV peptide | NV2.3509
LRE peptide | NV2.12847
GWA peptide | NV2.5029
QIa | NV2.5226
IPIa/IPFa | NV2.25578
HLSa/SNIa/NTVa | NV2.19361
WFSa | NV2.16562
CCa | NV2.24065
FFKAa | NV2.12163
GLWa | NV2.11082
NRFa | NV2.23710
FRPa | NV2.11031
RPa | NV2.15163
QW peptide | NV2.18275
QWa | NV2.4017
QITRFa | NV2.23834
VRHa | NV2.15165
PRGa | NV2.16299
QGRFa | NV2.8437
LRWa−3 | NV2.10312
LRWa−2 | NV2.10313
LRWa−1 | NV2.10311
HIRa | NV2.8166
GLWL−b | NV2.23207
GLWL−a | NV2.23205
FLRNa | NV2.1448
PFHa−R.36 | NV2.20426
FRPa−RPa−R.248 | NV2.3638
QWa−R.69 | NV2.9996
QITRFa−R.196 | NV2.9618
VRHa−R.186 | NV2.3564
PRGa−R.32 | NV2.22136
PRGa−R.28 | NV2.1943
PRGa−R.223 | NV2.2307
PRGa−R.222 | NV2.1945
PRGa−R.221 | NV2.1941
PRGa−R.220 | NV2.512
PRGa−R.219 | NV2.511
PRGa−R.211 | NV2.1942
PRGa−R.210 | NV2.3314
PRGa−R.202 | NV2.21659
PRGa−R.200 | NV2.11164
PRGa−R.199 | NV2.21302
PRGa−R.198 | NV2.22132
QGRFa−R.70 | NV2.9922
QGRFa−R.234 | NV2.1352
LRWa3−R.204 | NV2.10076
LRWa2−R.213 | NV2.23402
LRWa1−R.19 | NV2.20941
LRWa−R.193 | NV2.10074
HIRa−R.29 | NV2.24982
HIRa−R.21 | NV2.23510
GLWL−R.18a | NV2.13124
FLRNa−R.26 | NV2.22838
FLRNa−R.187 | NV2.23421
FLRNa−R.230 | NV2.16286
FLRNa−R.197−i2 | NV2.9939
FLRNa−R.197−i1 | NV2.14466
pSC_DevSubset
PGCs_DevSubset
neurogland.all_DevSubset
gland.mucous_DevSubset
immune_DevSubset
cnidocyte_DevSubset
retractor muscle_DevSubset
endomesoderm.embryonic_DevSubset
gastrodermis_DevSubset
pharyngeal.ect_DevSubset
ectoderm.embryonic_DevSubset
epithelia.ect_DevSubset
Split Identity
% expressed
10
20
30
2.5
developmental
adults
0

Figure 5–figure supplement 1: Tissue-specific expression of neuropeptide precursors and neuropeptide receptors (GPCRs) in *N. vectensis* . Dotplot for tissue-specific expression of proneuropeptides and GPCRs. **P**roneuropeptides without a known receptor are also included. Red dots indicate expression in the developmental dataset, blue dots indicate expression in the adult dataset.

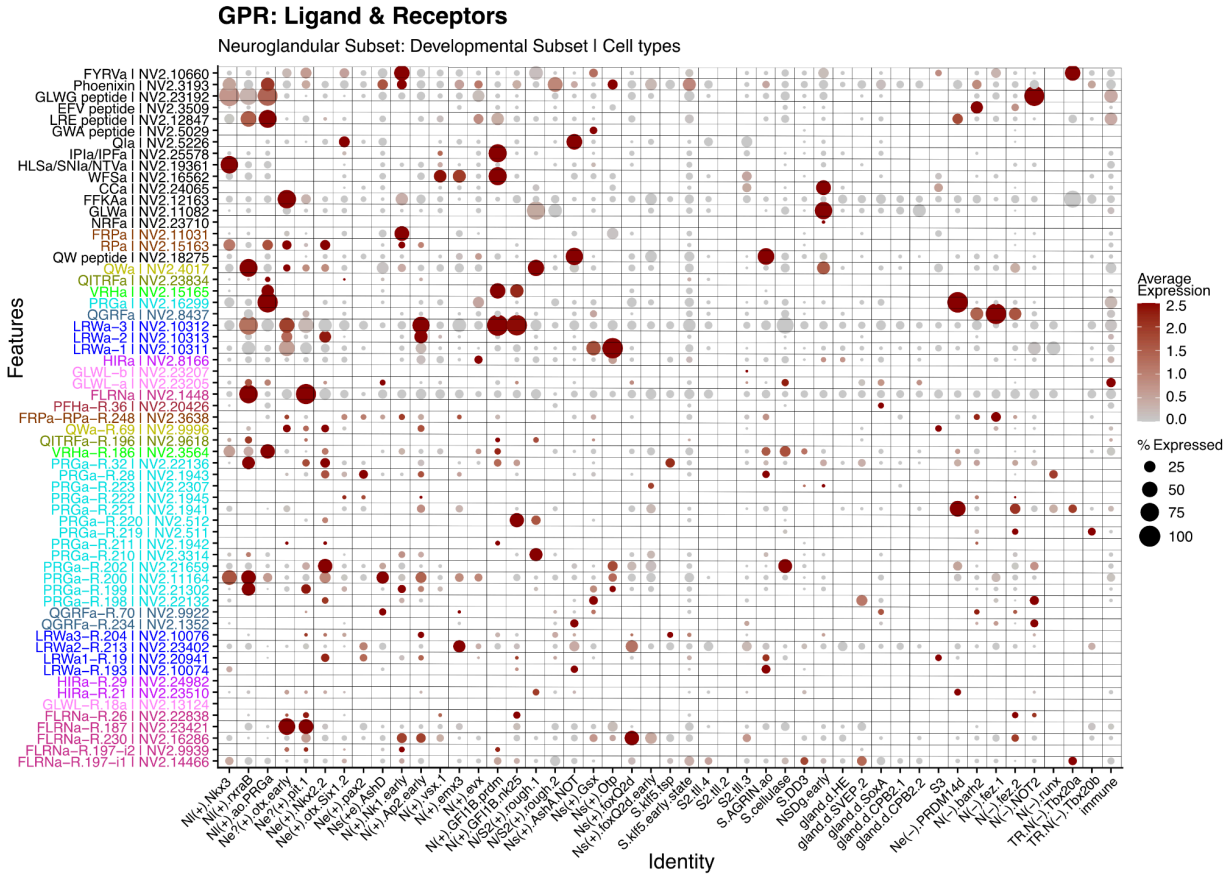

Figure 5–figure supplement 2: Expression of neuropeptide precursors and GPCRs in neuroglandular cell types in the developmental dataset. Dot size indicates percentage of cells expressing the corresponding gene, color intensity indicates average expression.

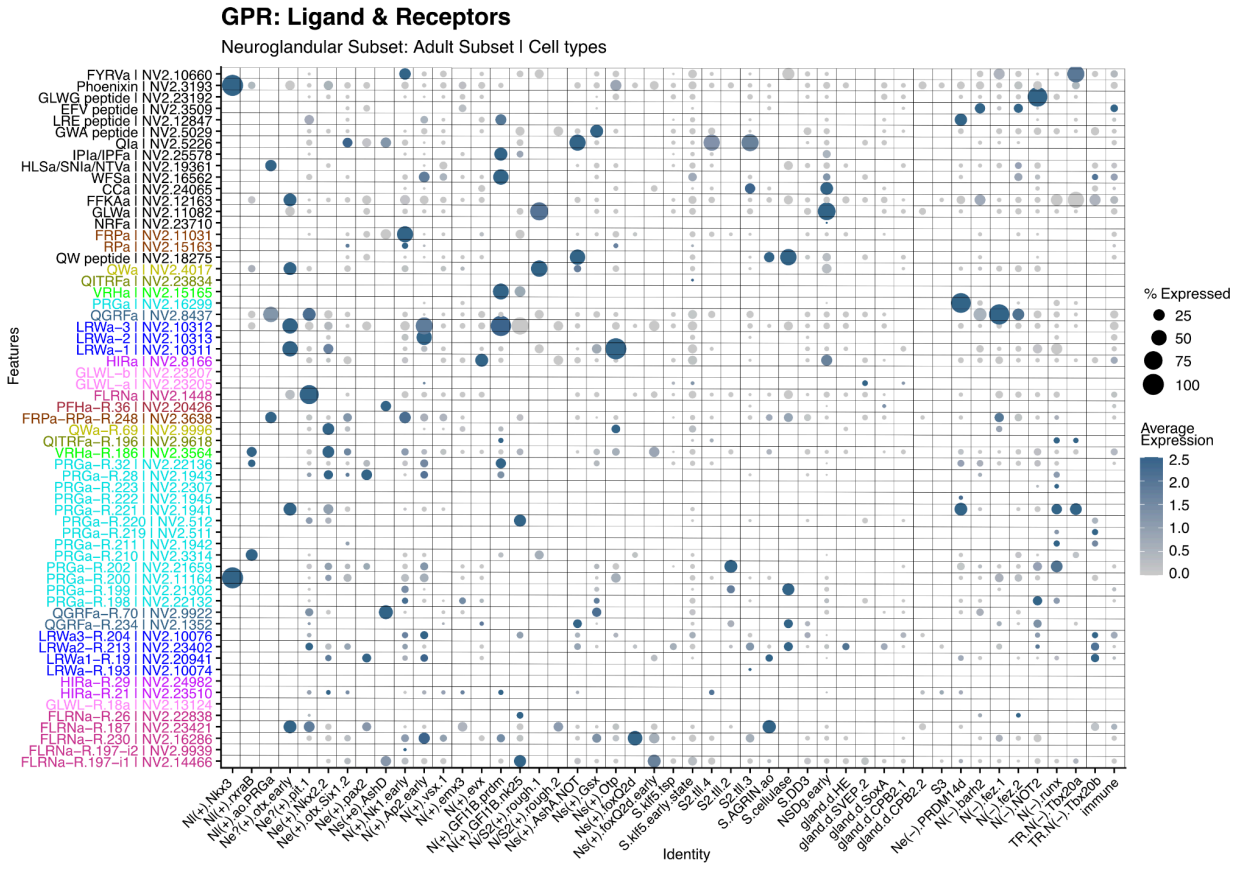

Figure 5–figure supplement 3: Expression of neuropeptide precursors and GPCRs in neuroglandular cell types in the adult dataset. Dot size indicates percentage of cells expressing the corresponding gene, color intensity indicates average expression.

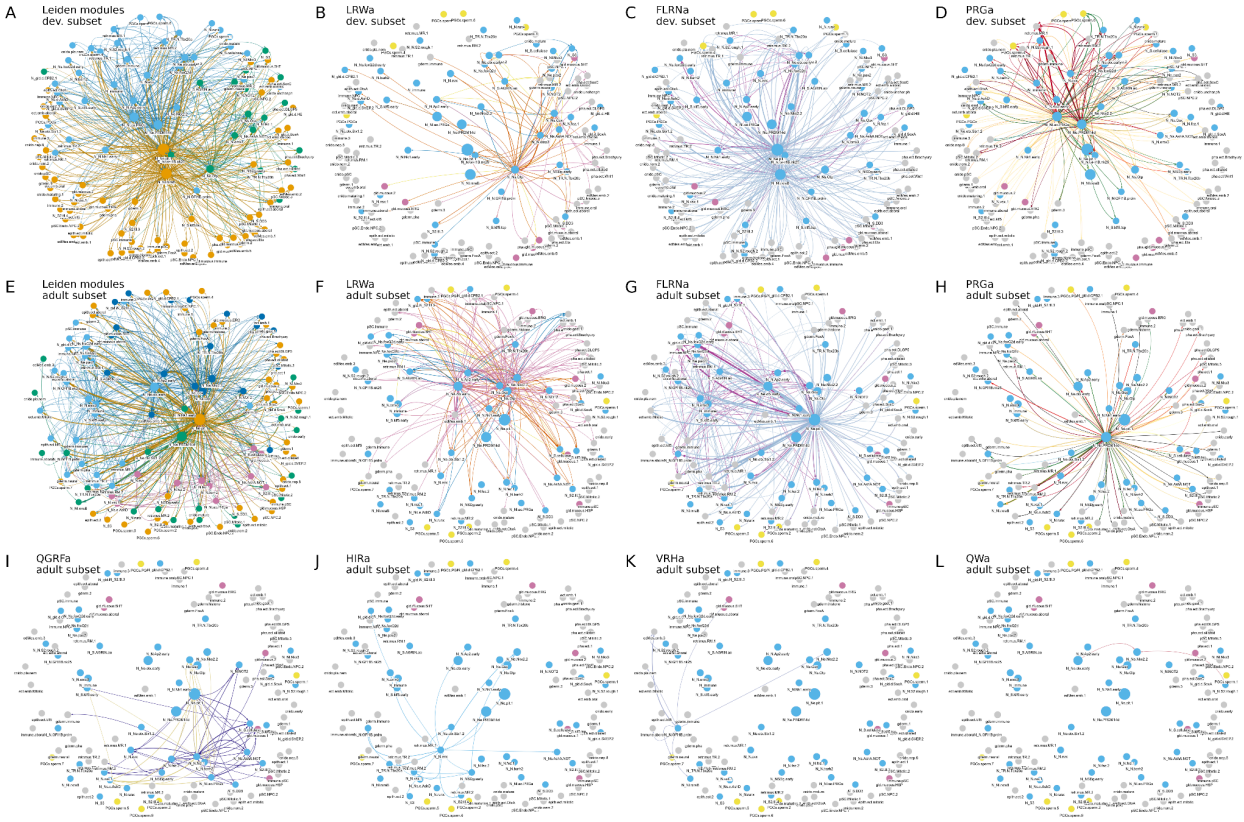

Figure 6–figure supplement 1: Multi-layer peptidergic connectomes in *Nematostella*. (**A**) Network of all peptide-receptor pairs for the developmental subset, coloured by network Leiden module. (**B-D**) Networks of LRWa (B), FLRNa (C) and PRGa (D) for the developmental subset. (**E**) Network of all peptide-receptor pairs for the adult subset, coloured by network Leiden module. (**F-L**) Networks of LRWa (F), FLRNa (G) PRGa (H), QGRFa (I), HIRa (J), VRHa (K) and QWa (L) for the adult subset. Nodes represent cell types, connections represent potential peptidergic signaling from neuropeptide-expressing cells to cells expressing one or more of the receptors for that neuropeptide. For peptides with more receptors, different colors represent different peptide-receptor signal channels (the different layers in the multi-layer connectome).

Reply to comments:
1- It was not clear why the phylogenetic analysis included non-validated GPCRs that clustered with the validated peptidergic receptors. Would restricting the phylogenetic analyses only to confirmed peptidergic GPCRs alter the topology of the tree and subsequent conclusions of independent expansion?

Thank you for this comment. In general, phylogenetic analyses become more robust if a larger diversity and fuller complement of sequences are included. With very sparse sampling, sequences that are homologous but not orthologous may be misleadingly grouped together, because intermediate sequences have been left out. For tree building, we thus did not want to focus only on experimentally validated receptors but also on all receptors that are phylogenetically related to the validated receptors. Only this approach can ensure a comprehensive exploration of the relationship of peptidergic receptors. The broader phylogenetic approach was also essential to identify orthologs to the experimentally validated Nematostella receptors across other cnidarian species.

2- Clearly, other neuropeptide signaling systems in cnidarians remain to be discovered but this paper represents a huge step forward.

We appreciate this assessment of the paper. We agree that many systems remain to be discovered. Our paper will also help with the identification of further receptors both in Nematostella as well as other cnidarian species. Please note that we have made specific receptor-ligand predictions for several cnidarian species based on our phylogenetic analysis. Our phylogenies could also help prioritize the study of the remaining orphan Nematostella GPCRs.

3- There are limitations in what can be interpreted from single cell transcriptomic data but the data nevertheless provide the foundations for future studies involving i). detailed anatomical analysis of neuropeptide and neuropeptide receptor expression in N. vectensis using mRNA in situ hybridization and/or immunohistochemical methods and ii). functional analysis of the physiological/behavioral roles of neuropeptide signaling systems in N. vectensis

We fully agree with this comment. The analysis of the available single-cell sequence resources clearly represents only the first step of anatomical and functional analyses. Our aim was to place the identified peptide-receptor interactions into a whole-organism context with cell type resolution, to highlight the potential complexity of peptidergic signaling in this organism and to facilitate the exploration and conceptualisation of our biochemical screen.

Comments to authors

1. In future, when preparing manuscripts, please use page and line numbers; it makes the task below for reviewers much easier!

We appreciate the suggestion and will do this for future manuscripts.

2. In the abstract the term "extensively wired" is used. In the context of neuropeptide mediated volume transmission this may not be an appropriate term to use because use of the word "wired" is likely to be associated with point-to-point type classical synaptic transmission; "extensively connected" would be better.

Thank you for this comment. We have changed the text in the abstract to "extensively connected".

3. Introduction: Please change "seven-transmembrane proteins and show a slower evolutionary rate than proneuropeptide..." to "seven-transmembrane proteins that show a slower evolutionary rate than proneuropeptide..."

Changed.

4. Under the section "Creation of a Nematostella neuropeptide library, what is meant by "our regular expressions"? This needs to be rephrased to make it clearer what is meant.

We have now rephrased the relevant sentence to make our approach clearer.
"This predicted secretome was filtered with regular expressions to detect sequences with the repetitive dibasic cleavage sites (K and R in any combination) and amidation sites, using a custom script from a previous publication (Thiel et al., 2021)."
and later:
"Based on the MS data, we included the additional, non-dibasic N-terminal cleavage sites into our script that uses regular expressions to search for repetitive cleavage sites (Thiel et al., 2024) and re-screened the predicted secretome."

5. Under the section "Creation of a Nematostella neuropeptide library" the phrase "differ in the length of their N-terminus" needs to be changed to "differ in the length of their N-terminal region". The N-terminus is, as its name implies, one end of the peptide/protein so it can't have a length as such.

Changed.

6. Under the section "Analysis of metazoan class A GPCRs and selection of N. vectensis neuropeptide-receptor candidates",
Change:
"For a more detailed analysis, we then reduced our sampled species to the cnidarian, the bilaterian with experimentally confirmed GPCRs and Petromyzon marinus, and the two placozoan species (Figure 2B)."
To
"For a more detailed analysis, we then reduced our sampled species to cnidarians, bilaterians

with experimentally confirmed GPCRs and Petromyzon marinus, and two placozoan species (Figure 2B)."

Changed.

7. Under the section "Analysis of metazoan class A GPCRs and selection of N. vectensis neuropeptide-receptor candidates" - change "We re-run" to "We re-ran"

Changed.

8. Throughout the paper reference is made to a variety of neuropeptides that have or are predicted to have an N-terminal pyroglutmate. However, these are referred to without indicating this post-translational modification e.g. QGRFamide.
This should be corrected throughout the paper, in the text, and figures. Two abbreviations for pyroglutamate are used in the literature:
pQ, which shows that the encoded amino acid is Q (Glutamine)
pE, which shows that the post-translationally modified amino-acid is glutamate (E)
In the neuropeptide field, pQ seems to be more widely used than pE, so our recommendation would be to use pQ.

In the revised version we now write pyroQ whenever we refer to the actual peptide. We now only use the peptide name without indicating this modification when we refer to the precursor of these peptides.

9. The title for Figure 5 is rather short and vague. A title like "Tissue-specific expression of neuropeptide precursors and receptors in Nematostella" seems more appropriate

We appreciate the reviewer's input, and we have made the change accordingly. The revised figure legend now reads: "Tissue-specific expression of neuropeptide precursors and receptors (GPCRs) in N. vectensis."

10. All of the figures in the paper have been saved in bitmap format (e.g. tiff), which means that the resolution of the figures may end up being poor in the published article. All of the figures in this paper should be saved in vector format (e.g. eps) so that there is no loss of resolution when the size of the file/figure is reduced.

We have now uploaded all figures in vector format (.eps or .pdf) to prevent any loss of resolution.

11. In Figure 3 - supplement 2 - the neuropeptides are referred to here as PRGamides and GPRGamides. Some consistency is needed here. And in Figure B, the G of one of the GPRGamides is not shown in black.

Thank you for spotting this mistake. We now give the correct peptide sequence in parenthesis

as "GPRGamide". We also highlighted the missing GPRGamide in the figure.

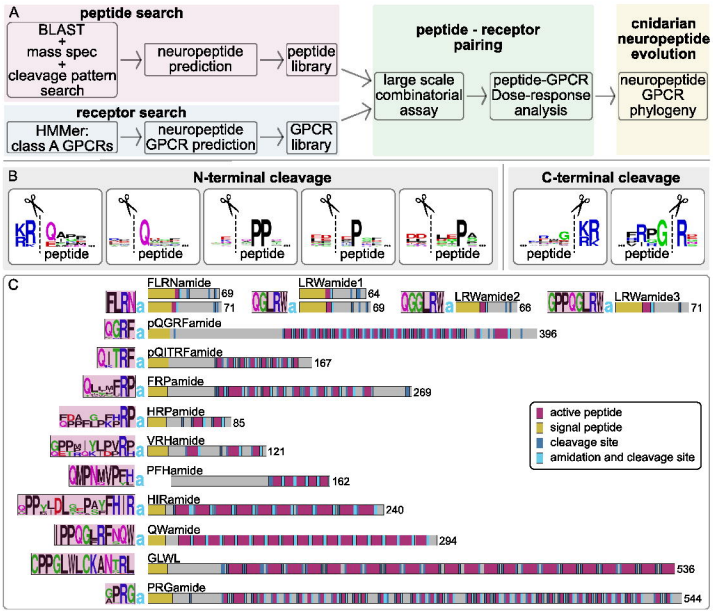
A
peptide search
BLAST + mass spec + cleavage pattern search
neuropeptide prediction
peptide library
receptor search
HMMer: class A GPCRs
neuropeptide GPCR prediction
GPCR library
peptide - receptor pairing
large scale combinatorial assay
peptide-GPCR Dose-response analysis
cnidarian neuropeptide evolution
neuropeptide GPCR phylogeny
B
N-terminal cleavage
C-terminal cleavage
peptide
C
FLRNamide
69
71
LRWamide1
64
69
LRWamide2
66
LRWamide3
71
pQGRFamide
396
pQITRFamide
167
FRPamide
269
HRPamide
85
VRHamide
121
PFHamide
162
HIRamide
240
QWamide
294
GLWL
536
PRGamide
544
active peptide
signal peptide
cleavage site
amidation and cleavage site

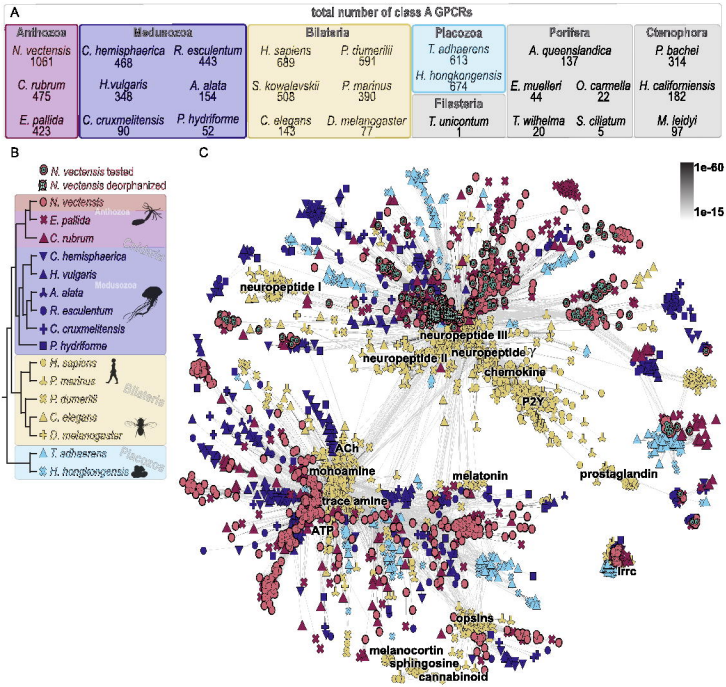
A
total number of class A GPCRs
Anthozoa
N. vectensis 1061
C. rubrum 475
E. pallida 423
Medusozoa
C. hemisphaerica 468
R. esculentum 443
H.vulgaris 348
A. alata 154
C. cruxmelitensis 90
P. hydriforme 52
Bilateria
H. sapiens 689
P. dumerilii 591
S. kowalevskii 508
P. marinus 390
C. elegans 143
D. melanogaster 77
Placozoa
T. adhaerens 513
H. hongkongensis 674
Filasteria
T. unicontum 1
Porifera
A. queensland ica 137
E. muelleri 44
O. carmella 22
T. wilhelma 20
S. ciliatum 5
Ctenophora
P. bachei 314
H. californiensis 182
M. leidyi 97
B
N. vectensis tested
N. vectensis deorphanized
Anthozoa
N. vectensis
E. pallida
C. rubrum
Cnidaria
Medusozoa
C. hemisphaerica
H. vulgaris
A. alata
R. esculentum
C. cruxmelitensis
P. hydriforme
Bilateria
H. sapiens
P. marinus
P. dumerilii
C. elegans
D. melanogaster
Placozoa
T. adhaerens
H. hongkongensis
C
1e-60
1e-15
neuropeptide I
neuropeptide III
neuropeptide II
neuropeptide γ
chemokine
P2Y
ACh
monoamine
melatonin
prostaglandin
trace amine
ATP
irrc
opsins
melanocortin
sphingosine
cannabinoid

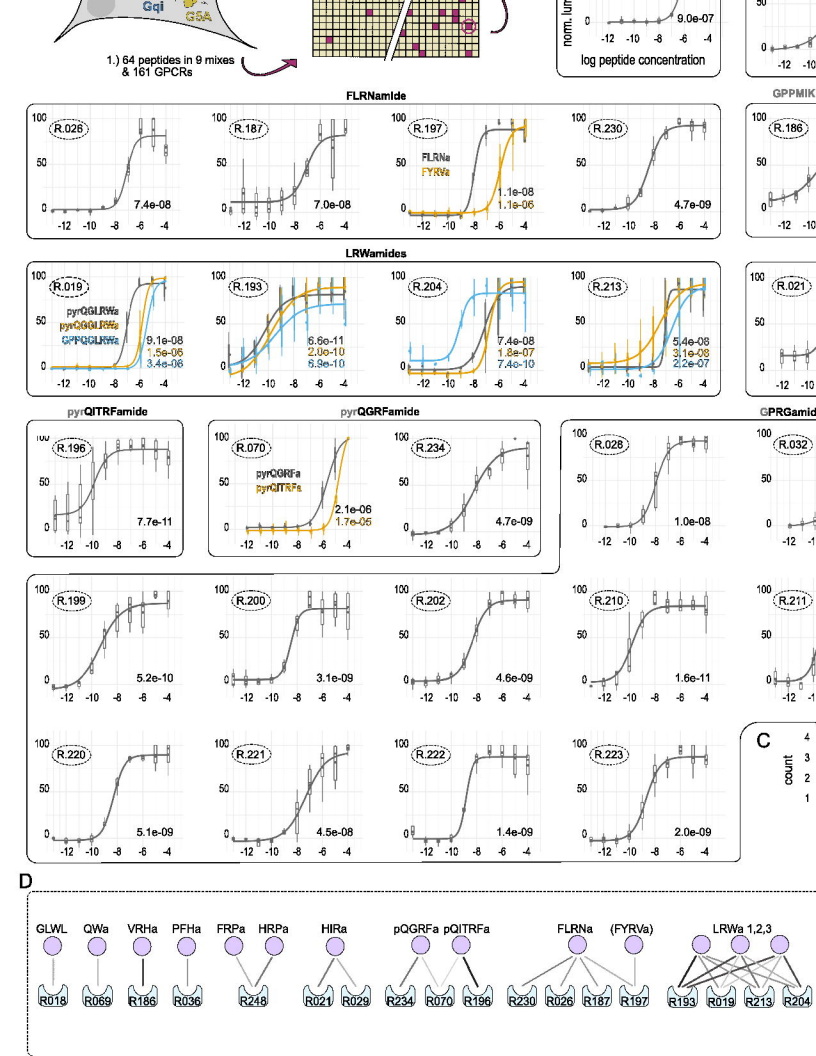
Gqi
G5A
1.) 64 peptides in 9 mixes
& 161 GPCRs
norm. lum
9.0e-07
log peptide concentration
FLRNamide
R.026
7.4e-08
R.187
7.0e-08
R.197
FLRNa
FYRVa
1.1e-08
1.1e-06
R.230
4.7e-09
GPPMIK
R.186
LRWamides
R.019
pyrQGLRWa
pyrQGGLRWa
GPRGQLRWa
9.1e-08
1.5e-06
3.4e-06
R.193
6.6e-11
2.0e-10
5.9e-10
R.204
7.4e-08
1.8e-07
7.4e-10
R.213
5.4e-08
3.1e-08
2.2e-07
R.021
pyrQITRFamide
R.196
7.7e-11
pyrQGRGamide
R.070
pyrQGRFa
pyrQITRFa
2.1e-06
1.7e-06
R.234
4.7e-09
GPRGamide
R.028
1.0e-08
R.032
R.199
5.2e-10
R.200
3.1e-09
R.202
4.6e-09
R.210
1.6e-11
R.211
R.220
5.1e-09
R.221
4.5e-08
R.222
1.4e-09
R.223
2.0e-09
C
count
D
GLWL
QWa
VRHa
PFHa
FRPa
HRPa
HIRa
pQGRFa
pQITRFa
FLRNa
(FYRVa)
LRWa 1,2,3
R018
R069
R186
R036
R248
R021
R029
R234
R070
R196
R230
R026
R187
R197
R193
R019
R213
R204

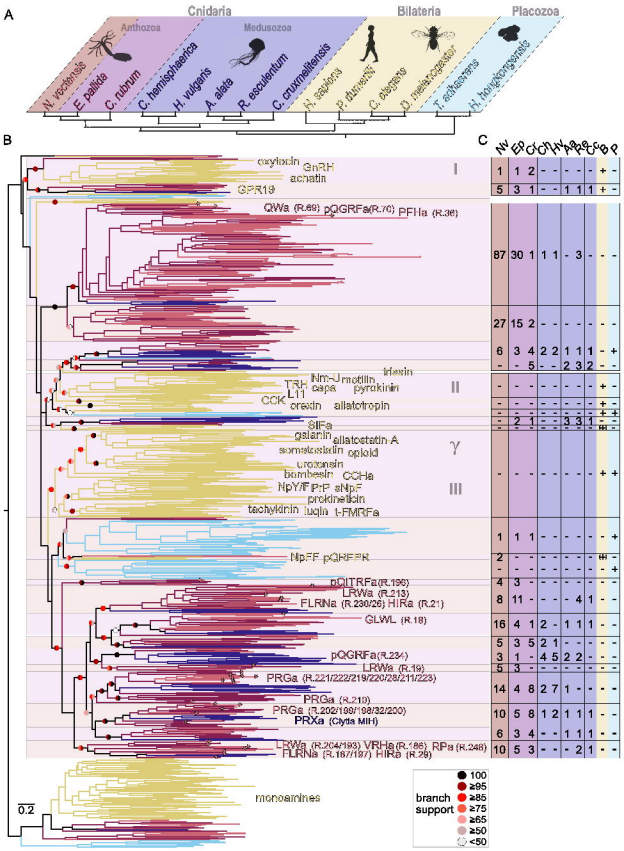
A
Cnidaria
Bilateria
Placozoa
Anthozoa
Medusozoa
N. vectensis
E. pallida
C. rubrum
C. hemisphaerica
H. vulgaris
A. alata
R. esculentum
C. cruxmeliensis
H. sapiens
P. dumerili
C. elegans
D. melanogaster
T. adhaerens
H. hongkongensis
B
C
Nv Ep Cr Cn Hv Aa Re Cc Ce P
oxytocin
GnRH
achatin
GPR19
QWa (R.69)
pQGRFa(R.70)
PFHa (R.36)
trissin
Nm-U
motilin
TRH
capa
pyrokinin
L11
CCK
orexin
allatotropin
SIFa
galanin
allatostatin A
somatostatin
opioid
urotensin
bombesin
CCHa
NpY/F
PrP
sNpF
prokineticin
tachykinin
luqin
t-FMRFa
NpFF
pQRFPR
pCITRFa(R.196)
LRWa (R.213)
FLRNa (R.230/26)
HIRa (R.21)
GLWL (R.18)
pQGRFa(R.234)
LRWa (R.19)
PRGa (R.221/222/219/220/28/211/223)
PRGa (R.210)
PRGa (R.202/199/198/32/200)
PRXa (Clytia MIH)
LRWa (R.204/193)
VRHa (R.186)
RPa (R.248)
FLRNa (R.167/197)
HIRa (R.29)
monoamines
I
II
III
γ
0.2
branch support
100
≥95
≥85
≥75
≥65
≥50
<50

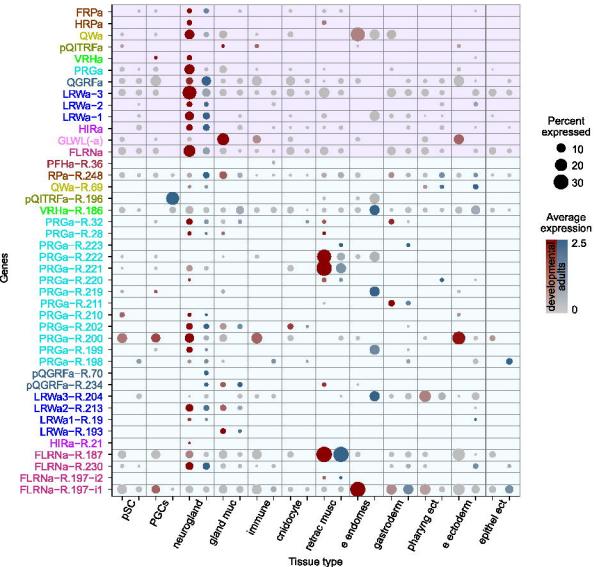

Genes
FRPa
HRPa
QWa
pQITRFa
VRHa
PRGa
QGRFa
LRWa−3
LRWa−2
LRWa−1
HIRa
GLWL(-a)
FLRNa
PFHa−R.36
RPa−R.248
QWa−R.69
pQITRFa−R.196
VRHa−R.186
PRGa−R.32
PRGa−R.28
PRGa−R.223
PRGa−R.222
PRGa−R.221
PRGa−R.220
PRGa−R.219
PRGa−R.211
PRGa−R.210
PRGa−R.202
PRGa−R.200
PRGa−R.199
PRGa−R.198
pQGRFa−R.70
pQGRFa−R.234
LRWa3−R.204
LRWa2−R.213
LRWa1−R.19
LRWa−R.193
HIRa−R.21
FLRNa−R.187
FLRNa−R.230
FLRNa−R.197−i2
FLRNa−R.197−i1
pSC
PGCs
neurogland
gland muc
immune
cnidocyte
retrac musc
e endomes
gastroderm
pharyng ect
e ectoderm
epithel ect
Tissue type
Percent expressed
10
20
30
Average expression
2.5
0
developmental adults

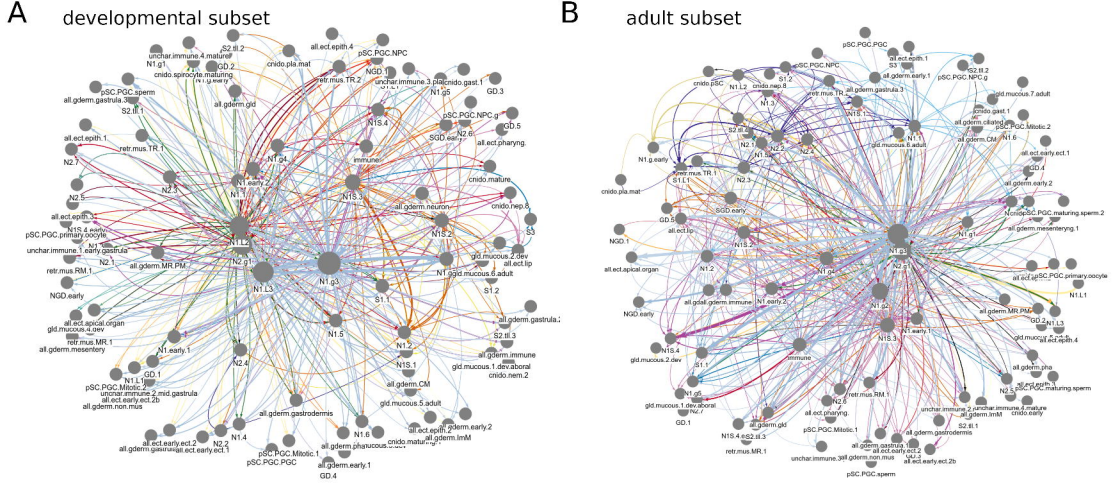
A
developmental subset
B
adult subset